Introduction

Since 2001 the Condensed Matter Physics Department (DPMC) in Geneva has been the leading house of the National Center of Competence in Research (NCCR) MaNEP "Materials with Novel Electronic Properties". This center, with the University of Geneva as host institution and a broad Swiss network, focuses its activities on research and development of novel materials with promising electronic properties. The NCCR allows a long term reinforcement of the research activities at the DPMC in the field of correlated oxide systems and related materials.

In 2002, two important events in our Department were the retirement of Prof. B. Giovannini and the nomination of Prof. T. Giamarchi, a specialist in the physics of low dimensional systems.

The DPMC has a long tradition in the studies of metallic materials with unconventional properties. In the last decade the interest of the department has been focused mostly on the understanding and development of high temperature superconductors and more recently superconducting MgB_2 as well as several classes of key novel materials, including colossal magnetoresistance compounds and ferro/dielectric oxides. All these materials have low electronic densities and a physics dominated by electronic interactions. The DPMC in Geneva has long standing experience in producing high quality materials in the form of single crystals, thin films and heterostructures, and tapes. The department also has a large expertise in the study of the physical properties of such materials. Several top class high quality experimental set-ups, including high magnetic field magnetotransport, transport under pressure, and specific heat measurements are installed. The department has also developed in the last years a novel area of expertise in local probe systems. These include Scanning Tunneling Microscopy and Spectroscopy, STM/STS, and Atomic Force Microscopy, AFM, that allow the characterization and study of materials on a nanoscopic scale. This report represents the research carried out at the DPMC, regardless of the source of funds. Part of this research was financed by the NCCR MaNEP and by the Swiss National Science Foundation project No 2000-65079.01.

Organization of the department

Director Jean-Marc Triscone

Faculty

Øystein Fischer
Tel. (022) 379 6270
e-mail: Oystein.Fischer@physics.unige.ch

Bernard Giovannini
Tel. (022) 379 6892
e-mail: Bernard.Giovannini@physics.unige.ch

René Flükiger
Tel. (022) 379 6240
e-mail: Rene.Flukiger@physics.unige.ch

Alain Junod
Tel. (022) 379 6204
e-mail: Alain.Junod@physics.unige.ch

Thierry Giamarchi
Tel. (022) 379 6363
e-mail: Thierry.Giamarchi@physics.unige.ch

Jean-Marc Triscone
Tel. (022) 379 6827
e-mail: Jean-Marc.Triscone@physics.unige.ch

Secretariat

Elisabeth Jeantin, Joséphine Mirabile, Nicole Nguyen

Department facilities

Computing Service: Ivan Maggio-Aprile
Helium: Gregory Manfrini and Spiros Zanos
Electronics: André Dupanloup, Patrick Magnin and Edouard Perréard
Teaching support: Charly Burgisser, Gérard Drocco, Yves Joly

University of Geneva
Department of Condensed Matter Physics
24 quai Ernest-Ansermet
1211 Geneva 4
Switzerland
Phone: +41 22 379 6511/6224/6264
Fax: +41 22 379 6869
Web site: http://dpmc.unige.ch

Research groups

Nanoscopic studies of superconductors and other interacting electron systems

Professor	Øystein FISCHER
MER	Michel DECROUX, Alfred MANUEL
Postdocs	Louis ANTOGNAZZA, Morten ESKILDSEN, Isabelle JOUMARD, Edmond KOLLER, Olivier KUFFER, Martin KUGLER, Ivan MAGGIO-APRILE, Serge REYMOND
PhD students	Cédric DUBOIS, Bart HOOGENBOOM[1], Pierre LEGENDRE[2], Giorgio LEVY DI CASTRO[3], Silvia SEIRO[4], Emmanuel TREBOUX
Diploma students	Cédric GOETSCHMANN, Nathan JENKINS[5]
Electronics Engineer	Laurent STARK
Technicians	Paul-Emile BISSON, Jean-Gabriel BOSCH, Arthur STETTLER

[1]until 31.08.02; [2]from 01.10.02; [3]from 01.06.02; [4]from 01.11.02;[5]from 1.10.02

Applications of superconductivity

Professor	René FLÜKIGER
Postdocs	Concetta BENEDUCE[1], Nicholas CLAYTON[2], Hiroki FUJII [3], Vincent GARNIER, Enrico GIANNINI, Reynald PASSERINI[4], Igor SAVYSYUK[5], Hongli SUO, Pierre TOULEMONDE[6]
PhD students	Nicolas MUSOLINO, Michael SCHINDL, Carmine SENATORE[7], Grégoire WITZ
Technicians	Patrick CERUTTI, Simon HUGI

[1]until 31.01.02; [2]from 01.05.02; [3]from 01.10.02; [4]until 31.08.02; [5]until 31.10.02; [6]until 31.08.02; [7]from 01.11.02

Theory of Condensed Matter

Professor	Thierry GIAMARCHI[1]
MER	Thomas JARLBORG[2]
Postdocs	Christophe BERTHOD[2], Carlos BOLECH GRET[2], Alberto ROSSO[3]

[1]from 01.07.02; [2]from 01.10.02; [3]from 01.09.02

Theory and numerical physics

Professor	Bernard GIOVANNINI[1]
MER	Thomas JARLBORG[1]
Postdoc	Christophe BERTHOD[1]

[1]until 30.09.02

Specific heat and magnetocaloric effect of metals and superconductors

Professor	Alain JUNOD
Postdoc	Frédéric BOUQUET, Tomasz PLACKOWSKI[1], Ilya SHEIKIN[2]
PhD student	Yuxing WANG
Technician	Aldo NAULA

[1]from 01.02.02 until 31.07.02; [2]until 31.10.02

Growth and electronic properties of unconventional metal and oxides

Professor	Jean-Marc TRISCONE
MER	Didier JACCARD
Postdocs	Albin DE MUER, Sarin KUMAR, Kei TAKAHASHI[1]
PhD students	Stefano GARIGLIO, Alexander HOLMES, Céline LICHTENSTEIGER[2]; Daniel MATTHEY, Patrycja PARUCH
Technicians	Renald CARTONI, Daniel CHABLAIX
Diploma student	Nicolas STÜCKI

[1]from 01.04.02; [2]from 01.02.02

Nanoscopic studies of superconductors and other interacting electron systems

Øystein FISCHER

Research summary

The group carries out research in the field of materials where strong interactions among the conduction electrons play an essential role. In this class of materials one finds superconductors, magnetic systems, and materials with other phase transitions. The group investigate such materials using two experimental tools : Scanning tunneling microscopy and spectroscopy on one hand and the fabrication and study of thin films multilayers and other artificial structures on the other. The scanning tunneling microscope (STM) is a powerful tool which offers the opportunity to perform imaging as well as spectroscopy with atomic resolution on conducting and semiconducting surfaces. Our group has a large experience in scanning tunnelling spectroscopy (STS) studies of high temperature superconductors, whereby we have uncovered some of their unusual electronic properties, such as gap values, pseudogaps features, and localised states in the vortex cores. Transport properties are also being investigated. By operating the STM in a scanning tunnelling potentiometry (STP) mode, we study the local transport properties of manganites. The group has a long standing expertise in the fabrication and study of thin films and heterostructures. This year we have continued our study tunneling spectra on high temperature superconductors and MgB_2. We have also carried out studies of the relation of strain, oxygen concentration and thickness in thin Nd123 films. We also report new results on the fault current limiter and on the development of an experiment to observe local I-V characteristics on high current carrying thin films.

Tunnelling spectroscopy of novel super-conductors

For the study of high-T_c superconductors, we often use scanning tunnelling spectroscopy as primary experimental tool. Complementary to our experimental work on $Bi_2Sr_2CaCu_2O_{8+\delta}$, we have performed numerical simulations to better understand the nature of the measured tunnelling spectra, for various oxygen dopings. In particular, we distinguish between the influence of tunnelling matrix elements, of band structure features (van Hove singularities), and of electronic effects directly related to high-T_c superconductivity. An additional, intriguing ingredient is the collective mode observed in neutron scattering experiments.

Using angular resolved photoemission (ARPES) and neutron scattering data that have only recently become available, we have managed to reproduce the experimental spectra in great detail. From the comparison between experimental and numerical results, we conclude that van Hove singularities considerably contribute to the asymmetry in the spectra and to the height of the coherence peaks. Interaction with a collective mode can explain the "dip-hump" next to the coherence peaks, and also the short lifetime of high-energy quasiparticles. However, in general, the quasiparticle lifetime appears an order of magnitude longer in tunnelling than in ARPES. Finally, the tunnelling matrix elements do not show high anisotropy.

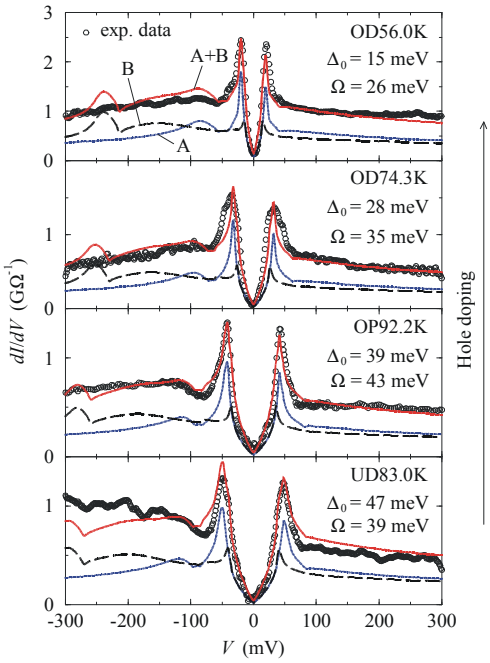

Fig.1.Experimental and calculated tunneling spectra of $Bi_2Sr_2CaCu_2O_{8+\delta}$, for different oxygen dopings. Shown are the data for both bands at the Fermi level, and their sum. Δ_0 indicates the superconducting gap, Ω the energy of the collective mode.

For more details and further reading, see B. W. Hoogenboom, Ph.D. thesis n° 3381 (2002); B. W. Hoogenboom *et al.*, cond-mat/0212329.

Two-band, two-gap superconductivity in MgB_2 was firmly established in 2002 by work in our group as well as by many others. In this respect it was important to realize that the observation of the larger of the two superconducting energy gaps depends crucially on the tunneling direction, as shown in Fig. 2.

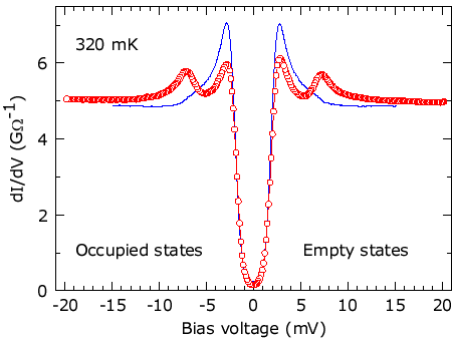

Fig. 2. Superconducting spectra of MgB_2 at 300 mK tunneling parallel to the c axis (blue line) and parallel to the basal plane (red circles).

In one of the spectra, obtained by tunneling parallel to the crystalline basal plane, two gaps with coherence peaks at 3 meV (π band) and 7 meV (σ band) are evident. Tunneling perpendicular to the basal plane only a single gap is seen. The sensitivity on the tunnel direction of the large gap, is due to this being associtaed with a 2D part of the Fermi surface.
We have performed vortex imaging in MgB_2 tunneling parallel to the *c* axis. Fig. 3. shows two examples of such images.

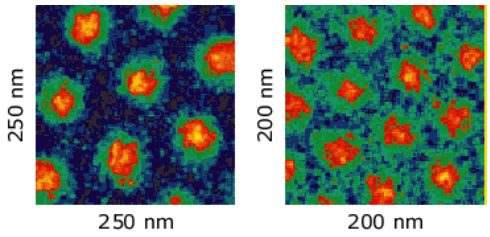

Fig. 3. Vortex images in MgB_2 at 0.2 T (left) and 0.5 T (right), tunneling parallel to the c axis. The color scale (different for each image) corresponds to the zero bias conductance.

With this tunnel direction we selectively measure the vortices in the π band. Measurements like these have allowed us to draw several conclusions, the most important being the existence of separate coherence lengths for the σ and π bands, and a very large degree of vortex core overlap in the π band already at very low fields compared to H_{c2}. Based on this we were able to understand the unusual field dependence of the electronic specific heat (T-linear term).

For more details see M. R. Eskildsen *et al.*, Phys. Rev. Lett. **89**, 187003 (2002); M. R. Eskildsen *et al.* Physica C **385**, 169 (2003). See also activities of Prof. A. Junod.

Potentiometry of Manganite Films

The colossal magneto-resistance compounds have recently gained considerable interest, because of their striking properties and their potential technological applications. However, the microscopic mechanisms responsible for their exceptional transport properties are far from being understood.

Electronic phase separation (PS) has been predicted for hole-doped manganites, involving the coexistence of separated ferromagnetic-metallic and insulating microscopic phases. We use STP to map the distribution of the electrical potential induced by a current flow, and to probe the local electronic transport of manganite thin films with a nanometer spatial resolution.

We have previously shown the absence of electronic or chemical mesoscopic PS in the manganite compound $La_{0.7}Sr_{0.3}MnO_3$ at room temperature on a 500 nm scale. We have started a study on $La_{0.7}Ca_{0.3}MnO_3$ (LCMO) in order to probe the existence of a PS in other optimally doped manganites. An epitaxial 53 nm thick LCMO film annealed in situ show a highly linear potential drop at room temperature (well above T_c) as shown in the second image of Fig.4.

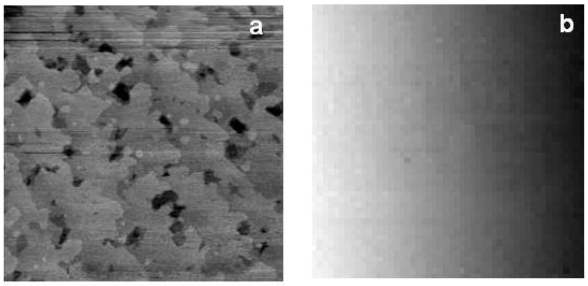

Fig.4. Topographic (a) and potentiometric (b) 500x500nm^2 images of a 53nm LCMO/STO thin film acquired with an applied electric field of 16V/mm. Gray scale : a) 6 nm, b) 6.2 mV

At room temperature, there is no evidence for PS at this scale. First low temperature STP measurements are under progress to probe the existence of PS near T_c (~250K) in LCMO.

For more details and further reading, see B. Grévin *et al.*, Appl. Phys. Lett. **80**, 3979 (2002).

Fault current limiter

Fault current limiter (FCL) are devices which limit the current, in an electrical network, during a short circuit. We are currently working on superconducting thin films based FCL, which are in fact a meander of Au/YBCO/CeO heterostructure on a 2" wafer.
In the previous report we have presented a particular design of the meander which improves the performance of the FCL. The idea behind our design is to split and uniformly distribute the initial dissipative length along the meander. This is done by locally decreasing the width of the line (and therefore the critical current), i.e. by including constrictions in the meander, as shown in figure 1. Their total length has to be chosen in order that only the constrictions are switching at the beginning of the short circuit for the maximum applied voltage. Using this design we have successfully tested a 3kW (300V-10A) FCL.

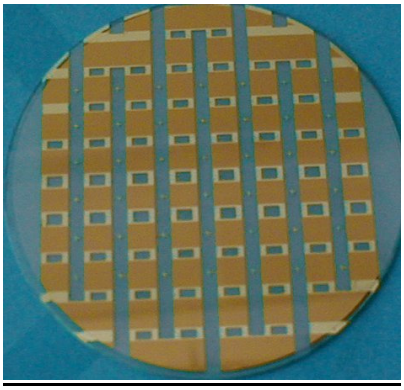

Fig 5: New design of the meander. An additional gold layer is grown on the constrictions in order to decrease their resistance.

During this year we have further improved the design of the meander with the aim to reduce the power density sustained by the wafer. We took into account the observed behavior of a YBCO line during a short circuit: after the usual initial peak current, the line is acting as a current source during the first 20-40µs and as a voltage source at longer time, where the current decreases due to the propagation of the dissipative region and the increase of its temperature. In term of power density P_s this means that, at the beginning of the short circuit, P_s is proportional to the resistivity ρ of the line (current source) whereas P_s goes like 1/ρ at longer time (voltage source). This suggests that reducing the sustained power at both short and longer time is contradictory. However thanks to the constrictions in the line, we can propose an elegant way to solve this conflict. Since only the constrictions are switching during the first µs, the power sustained by them can be decreased by decreasing their resistance. This is done by increasing the thickness of the gold layer on the constrictions, which requires an additional step in the lithographic process. On the other hand a thinner gold layer is grown on the connecting paths which increases their resistance and then decreases the sustained power at longer time. The final design is shown in Fig.5; the thickness of the gold layer is 135nm on the constrictions and 50nm on the connecting paths. A thin (15nm) silver layer is also grown on the constrictions for a better contrast during the lithographic process. This wafer has been successfully tested, for periods as long as 100ms, at 5kW (300V-16A). In collaboration with ABB we have filled up a patent claim for this new design.

Local observation of I-V characteristics

We are developing an experiment to measure the I-V characteristics locally and at low temperature. The aim is to acquire an instantaneous potential profile of a sample carrying a current and in particular to directly image the formation of highly dissipative domains in HTC thin films, which are at the origin of the current induced transition into the normal state in FCL. The design is essentially based on the scanning tunneling microscope used in the group. However it differs by two points: first a carriage driven inertially allows for extended motion along an horizontal axis and second a silicon tip with a metallic coating is mounted on a cantilever (like for AFM), enabling a "soft touch" to the sample surface.
Using this instrument, we measured the instantaneous potential profile of a platinum film modified by Joule heating along a sample with a constriction. Measurement at low temperature have also been performed. Presently we are working on connecting a HTC thin film. In these compounds the difficulty comes from the high contact resistance, due to the insulating character of the surface after air exposure.

Does strain really affect the properties of NBCO ? What happens with reduced thickness ?

Superconducting films of $Nd_{1+x}Ba_{2-x}Cu_3O_{7+\delta}$ show a decrease of T_c with reduced thickness. This phenomenon can in principle be due to various effects: change in the oxygen proportion (doping), strain effects or transition to a 2D behaviour. In order to clarify this question we made various measurements on two sets of samples: one with optimal doping conditions and varying thickness (from 3.6 nm to 100 nm), and one with various reduced oxygen concentrations at a fixed thickness (100 nm).

By comparing the resistivity measurements (cf. fig 6), we see that the two series have different behaviours, showing different relations between $\rho(T)$ and T_c.

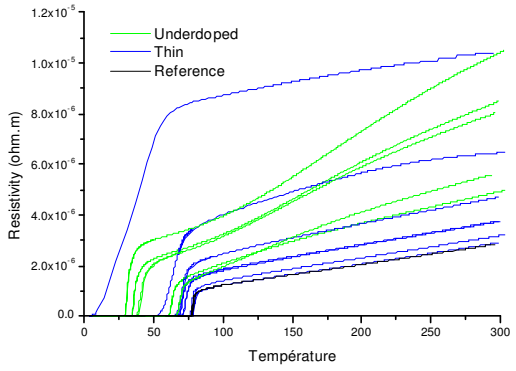

Fig. 6 : Resistivity as a function of temperature for thin samples (3.6 nm → 100 nm) and underdoped samples. Reference is for 100 nm optimally doped.

We also made Hall effect measurements on these samples, to obtain information on the carrier density. These measurements are still running: but so far confirms the expected dependence of T_c on doping. Nevertheless, the variation of the inverse Hall number with temperature is linear for the first set of samples whereas it deviates from linearity in the case of the underdoped samples in the second set.
X-ray measurements gave us a more spectacular result. We measured very precisely the c-axis parameter of our samples. We know that oxygen brings carriers (holes) to the system as well as it changes lattice parameters. So, if we consider that the T_c is only dependent on the oxygen doping, it should have one unique relation to the c axis value, as previously seen in bulk samples. This is what is observed for underdoped thick samples (green line on fig. 7).

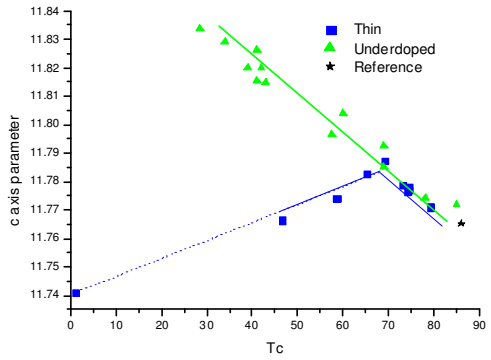

Fig. 7: c axis parameter versus T_c for thin samples (3.6 nm → 100 nm) and underdoped samples

But thin samples from the first set of samples deviate from this line (Fig. 7 blue line), which means that their decrease of T_c is not only due to oxygen depletion.

The conclusion is that the T_c drop is related to strain or to a 2D fluctuations (Berezinskii-Kosterlitz-Thouless). This 2D effect could very well explain the dramatic broadening of superconducting transition observed below 6 nm, but is unlikely to account for the behaviour of samples up to 100 nm. Consequently the T_c behaviour of thin films is certainly influenced by all three parameters : oxygen doping, strain and 2D fluctuations.

Superconducting behavior of $PrBa_2Cu_3O_{7-\delta}$ in bilayers

Among the isostructural $ReBa_2Cu_3O_{7-\delta}$ (R=rare earth element) superconducting compounds, $PrBa_2Cu_3O_{7-\delta}$ (PrBCO) is exceptional for its insulating behaviour. We are here studying the behaviour of thin PrBCO films in contact with thin superconducting films of $NdBa_2Cu_3O_{7-\delta}$. We are in particular interested in the proximity effect between the two.

Our preliminary studies, on PrBCO thin films, confirmed that their transport properties are very sensitive to the growth conditions. We therefore carefully control the growth conditions. Based on these results we have in this project studied the c-axis transport of PrBCO/NdBCO bilayers. These heterostructures show a striking behaviour. As the temperature decreases the resistance of the sample shows, for thickness of the PrBCO layer much larger than the NdBCO coherence length, a double superconducting transition, as reported in fig.8.

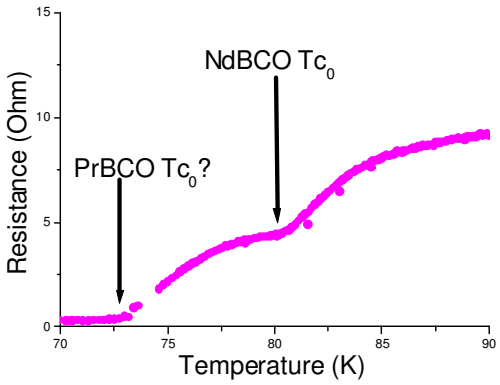

Fig. 8 : Resistance as a function of the temperature for a PBCO/NdBCO bilayer.

The first transition is doubtless associated with the NdBCO layer. The origin of the second transition is still not clear. Is it related to the PrBCO layer and if yes, does this mean that there is a giant proximity effect?
To clarify the origin of this peculiar behaviour we are currently studying the systematics of the occurrence of this phenomenon.

Applications of superconductivity

René Flükiger

Research summary: The research in our group is centred on the formation conditions of superconductors, on crystal growth and on the analysis of metallurgical and physical properties, in particular the critical current density. A new research activity on thermodynamics of volatile compounds is now possible thanks to the development of a High Pressure Differential Thermal Analysis apparatus working at gas pressure up to 2 kbar and T≤1200°C. The direct Bi,Pb(2223) phase formation from the melt (up to 70% volume) was observed for the first time by means of High Temperature *In-Situ* Neutron Diffraction, both in bulk samples and Ag-sheathed tapes. This result opens new possible routes for the formation of Bi,Pb(2223) filaments under equilibrium conditions. Substantial improvements in the single crystal growth of Pb-free Bi(2223) have been obtained. Crystals grown by the Travelling Solvent Floating Zone method are as large as 2x1x0.1 mm^3 and exhibit a sharp superconducting transition at T_c =109 ÷ 111 K, with ΔT_c = 1 K. MgB_2 single crystals up to 300 µm large were grown in Mg flux after melting a Mg + B mixture at T = 1200 - 1600°C and p = 3-4 GPa in a cubic anvil apparatus. A new heavily Pb doped and modulation-free phase has been found in the system $Bi_{2-x}Pb_xSr_2CaCu_2O_{8+y}$ and single crystals of this phase have been grown. A magnetic investigation on these crystals has shown that this new phase is responsible for the observed flux pinning enhancement in Bi,Pb(2212) superconductors.

New infrastructure

High pressure DTA prototype

An investigation of the unknown high-pressure phase diagram of the Bi-Pb-Sr-Ca-Cu-O system is made indispensable by the recent results on the positive effect of high pressure on the Bi,Pb(2223) phase processing.
For this purpose, a 3-sensor Differential Thermal Analyser (DTA) has been fabricated to work at high pressure under oxidising atmosphere. This prototype was installed in a Hot Isostatic Pressure furnace (HIP) allowing to operate up to T=1'200°C and p=2'000 bar (at a maximum oxygen partial pressure of $p(O_2)$=400 bar). After DTA calibration with gold and silver, thermodynamic studies on the high pressure phase diagram of the system Bi-Pb-Sr-Ca-Cu-O have been started.
This new HP-DTA prototype opens new perspectives in high pressure thermodynamic studies of many other systems.

Thermodynamic Studies

Reversible melting and equilibrium phase formation of $(Bi,Pb)_2Sr_2Ca_2Cu_3O_{10+d}$

New *In-situ* high-temperature neutron diffraction studies have been carried on in order to further elucidate the decomposition and re-formation mechanism of the $(Bi,Pb)_2Sr_2Ca_2Cu_3O_{10+d}$ (Bi,Pb(2223) phase, searching for an *equilibrium* processing route for both bulk samples and Ag sheathed tapes. After having previously shown a partial Bi,Pb(2223) re-formation from the melt in Ag sheathed tapes, we have now performed new experiments at the SINQ Neutron Spallation Source (PSI, Villigen). On samples sealed in quartz tubes (to reduce Pb losses), we have confirmed the incongruent melting of the Bi,Pb(2223) phase into $(Ca,Sr)_2CuO_3$,

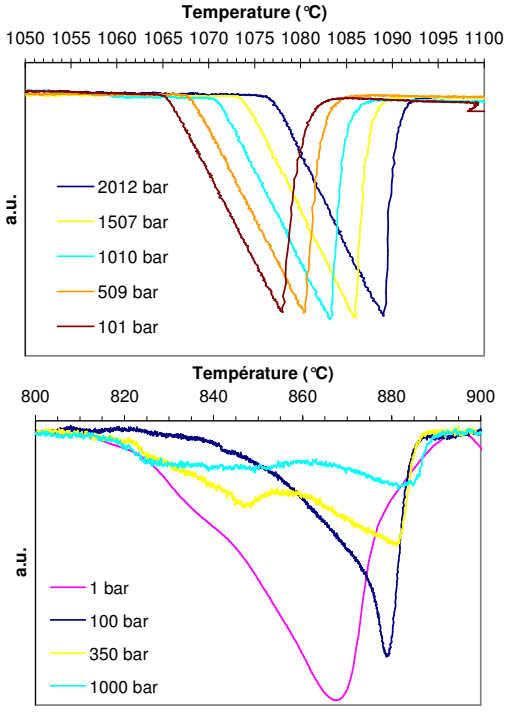

Figure 1: DTA measurements at various pressures: (a) Gold melting point under pure Ar; (b) Bi,Pb(2223) green tapes under 0.07 bar of O_2 (balance: Ar).

$(Sr,Ca)_{14}Cu_{24}O_{41}$ and a Pb,Bi-rich liquid phase. A direct Bi,Pb(2223) formation from the melt was now observed in bulk samples, too, ≈ 70% of Bi,Pb(2223) being recovered within 10 hours at 862°C after melting at 894°C (Fig.1). This is a considerable progress with respect to our earlier results. In particular, Bi,Pb(2212) was not found

to participate to the equilibrium re-formation process. The appropriate conditions for Bi,Pb(2223) re-formation are extremely sensitive both to temperature and local Pb content. The present results open new perspectives in Bi,Pb(2223) processing for power applications.

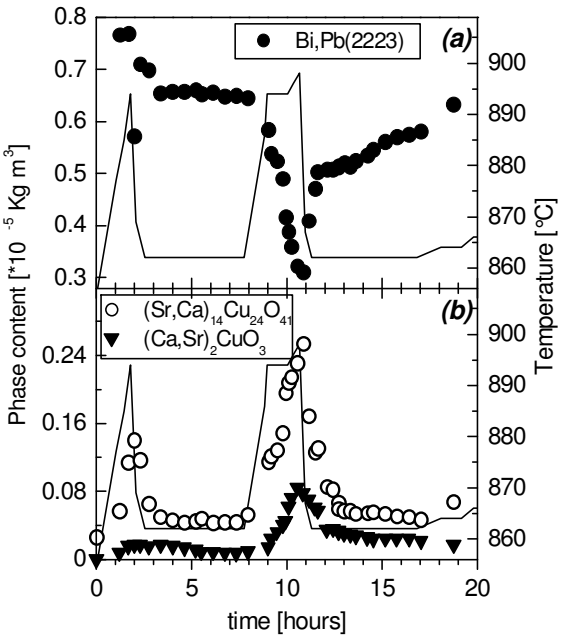

Figure 2: (a) Bi,Pb(2223) and (b) Ca_2CuO_3 and $(Sr,Ca)_{14}Cu_{24}O_{41}$ phase content as a function of time during partial melting and re-formation.

Phase formation, thermodynamics and superconducting properties of Pb-free Bi(2223)

In spite of the difficulties to synthesise pure Pb-free Bi(2223) samples, there is a renewed interest in this compound due to the observation of large grain growth in the Pb-free system. In addition, the problem of strong Pb and PbO losses is avoided. Pb-free pressed pellets with ~80% Bi(2223) phase have been synthesised, starting from home-made precursors. After crushing, the powders have been used for preparing Ag sheated monofilamentary and 37-filament tapes. As a result, almost pure well-crystalline Bi(2223) phase was obtained in the filament core after annealing at 850-860°C for 100 hours, both in air and in 7% O_2 atmosphere. The presence of Ag accelerates the grain growth and strongly decreases the reaction temperature, showing that Ag promotes the transient liquid formation. Large grains are merely observed at the filament/Ag interface, where Bi(2223) platelets as large as 50-100µm are commonly found. Very large platelets, ~300-500µm, are occasionally found as filament outgrowths in multifilamentary samples (Fig. 3). However, because of the inhomogeneous transient liquid formation and the crystallisation of secondary phases, poor grain connectivity is obtained in Pb-free Bi(2223) tapes. This leads to much lower J_c values compared to the Pb-doped Bi(2223) samples.

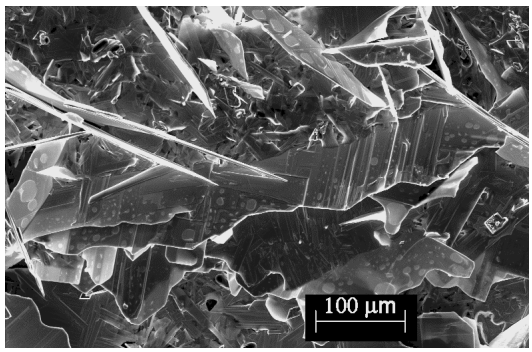

Figure 3: SEM picture of large filaments outgrowths (up to 500 mm) of Pb-free Bi(2223) grown in the Ag matrix of a multifilamentary tape.

Precursor powder preparation

A sol-gel method to prepare precursor powder has been developed. This chemical approach using nitric acid, ammoniac and EDTA (Ethylenediaminetetracetic acid) allows to prepare sizeable quantities of homogeneous, fine and reactive powder. These powders are currently used in our laboratory for experiments employing compositions not being commercially available, e.g. Pb-free single crystal growth and Ag-sheathed Pb-free Bi(2223) tape processing.

Crystal Growth

$Bi_2Sr_2Ca_2Cu_3O_{10}$ crystals

$Bi_2Sr_2Ca_2Cu_3O_{10}$ crystals have been grown using a Travelling Solvent Floating Zone technique (TSFZ) in a home-made image furnace equipped with two 400W halogen lamps. The furnace, already used in the past to grow Bi(2212) crystals, has been modified to reach the extraordinarily low floating zone velocities needed for Bi(2223) crystal growth. Crystals as large as $2\times1\times0.1$ mm^3 were obtained at growth rates of 60 µm/h (Fig. 4). The precursor rod consisted of a calcined sol-gel powder having a nominal composition $Bi_{2.1}Sr_{1.9}Ca_2Cu_3O_y$. The precursor rod was pre-melted to obtain a dense and homogenous feed rod for crystal growth experiments. A very stable and flat 3 mm high liquid zone was maintained over several weeks under flowing 7%O_2-93%Ar gas mixture. As-grown rods always contained both Bi(2212) and Bi(2223) crystals, the latter exhibiting a rather low superconducting transition

temperature (T_c = 102 K). After annealing at 500 °C in 100 bar O_2 atmosphere, T_C increased up to 111 K and a sharp superconducting transition (ΔT_c = 1 –2 K) was observed (Fig. 5).

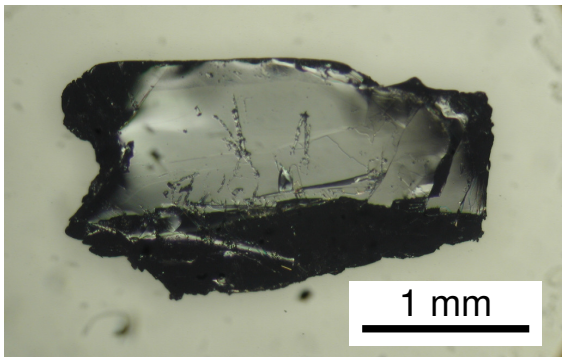

Figure 4: Bi(2223) single crystal

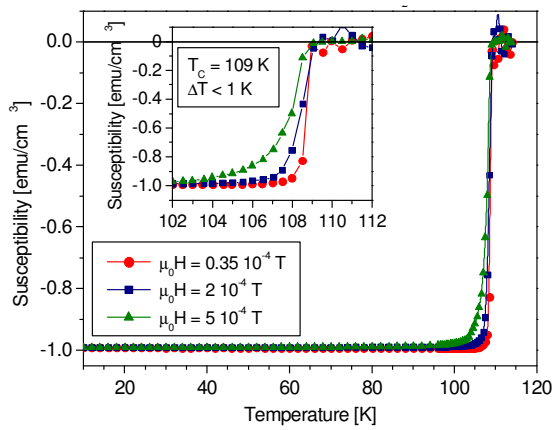

Figure 5: Superconducting transition of a Bi(2223) single crystal after post annealing in pure oxygen measured by a SQUID magnetometer.

MgB_2 crystals

MgB_2 single crystals were grown in a Mg flux using a high pressure technique. 200-300 µm large crystals were obtained after melting a precursor mixture of Mg and B at 1300-1600 °C at p = 3 - 3.5 GPa, followed by fast cooling. The overall starting stoichiometry was chosen in order to have an excess of liquid Mg acting as solvent for MgB_2. In order to prevent Mg from escaping and reacting either with oxygen or with the BN crucible, the precursor pellet was wrapped inside a Ta foil. No reaction between MgB_2 and Ta was found to occur below 1400 °C. After cooling, the samples show bright platelets dispersed in a matrix containing metallic Mg and other Mg-B secondary phases. A number of hexagonal MgB_2 crystals were successfully extracted from the matrix (Fig.6).
Without using the Ta foil, strong interactions between the sample and the BN crucible are observed and MgB_2 growth has to be controlled within the more complex Mg-B-N ternary system, where several intermediate ternary phases form. The use of Ta allows to remain in the simpler binary Mg-B system. In addition, we have found that crystal growth occurs at temperatures as low as 1250 °C.
Work is still in progress with the aim of optimising the experimental conditions to grow larger crystals. MgB_2 crystal growth is a very challenging problem, because of the inherent experimental difficulties, but is of great interest for the study of fundamental physical properties of this system.

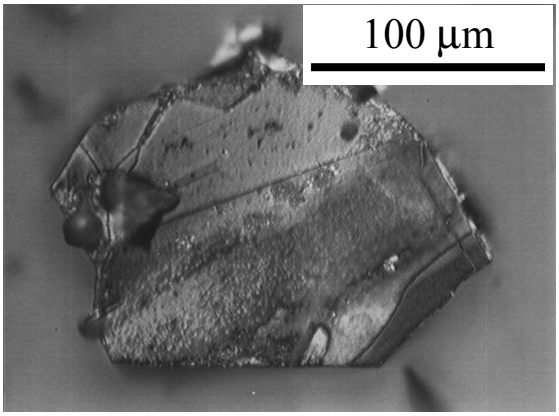

Figure 6: MgB_2 single crystal.

Enhanced Flux Pinning in Pb-Doped Bi-2212 Crystals: New Modulation-Free Phase

Modulation-free $Bi_{1.6}Pb_{0.4}Sr_2CaCu_2O_{8+\delta}$ single crystals (nominal: $Bi_{1.2}Pb_{0.8}Sr_2CaCu_2O_{8+\delta}$) have been grown for the first time by a slow cooling technique in home-made $BaZrO_3$ crucibles (crystal size 2 × 1 × 0.05 mm^3). The complete disappearance of the structural modulation has been observed by transmission electron microscopy (TEM) as well as by X ray diffraction. The superconducting properties of the new modulation-free phase (β phase) have been compared to those of undoped, modulated Bi(2212) crystals (α phase). Magnetisation measurements reveal that the irreversibility fields, $H_{irr}(T)$, and the relaxation rates, S, are noticeably improved for the modulation-free β phase. In addition, the lower critical field, H_{c1}, also reflect that the anisotropy factor ε is considerably reduced in the β phase.
The enhanced flux pinning properties in the modulation-free crystals are due to the enhanced coupling between Cu-O_2 planes in this anisotropic superconductor. The driving force behind the structural modulation is the lattice mismatch between the Bi-O layers and the perovskite blocks. To reduce the stress, excess oxygen is periodically inserted into the $(Bi\text{-}O)_2$ blocks, leading to an expansion of the Bi-Bi

distance. The substitution of Bi^{3+} by Pb^{2+} decreases this additional oxygen content. The amount of Pb necessary to obtain a modulation-free configuration in our crystals is in good agreement with the value predicted in the literature.

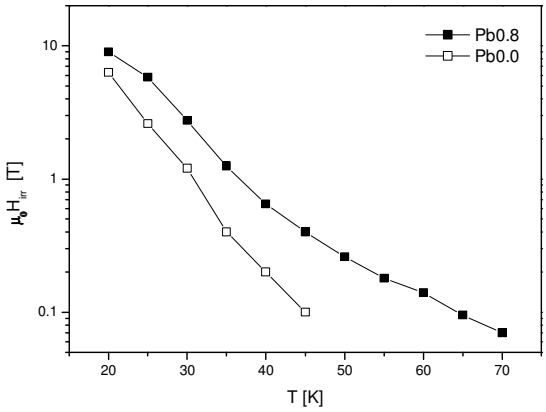

Figure 7: Irreversibility fields of a Pb-free crystal (α phase) and of a heavily Pb-doped crystal (β phase) obtained from magnetic measurements. The irreversibility field is increased in the modulation-free crystal.

Synthesis and characterisation of pure and doped MgB_2 superconductor

The effect of additives on the superconducting properties of MgB_2 has been investigated. Bulk, dense, pure MgB_2 and doped $(Mg_{1-x}A_x)B_2$ samples with A = Na, Ca, Cu, Ag, Zn and Al were studied for compositional ranges $0 < x < 0.20$. The effects on pinning properties and critical current were investigated, particularly for A = Aluminium. The samples were synthesised at high pressure–high temperature in a cubic multi-anvil press (typically 3.5–6 GPa, 900–1000 °C). They were characterised by X-ray Diffraction, Scanning Electron Microscopy and their superconducting properties were investigated by AC susceptibility, DC magnetisation and transport measurements in applied magnetic field. Only Al really substitutes on the Mg site. The other elements form secondary phases with B or Mg which do not act as pinning centres. Even if substitution of Al for Mg was successful, the effect of Al additions on H_{c2} remains small. Furthermore, the irreversibility fields remain unchanged as well as the critical current density. No positive effect was observed on the superconducting properties (T_c, J_c, H_{irr} and H_{c2}) of bulk MgB_2 samples for the other doping elements.

I_C versus strain measurements in Bi-2223 tapes

The amount of prestrain and the maximum value of the critical current of superconducting wires are important parameters in the design of high field magnets. In collaboration with B. Seeber and D. Uglietti (GAP-Supra), we have developed a new device (WASP) for the measurement of J_c under strain up to 17 T at currents up to 1000 A on 80 cm of wire, allowing for the first time a resolution of 0.1μV/cm for I_c. The WASP device has been widely used for measuring several kinds of superconducting wires and tapes. The results on the strain dependence of J_c and the exponential factor *n* for a multifilamentary Ag/Bi,Pb(2223) tape are shown in Fig.8.

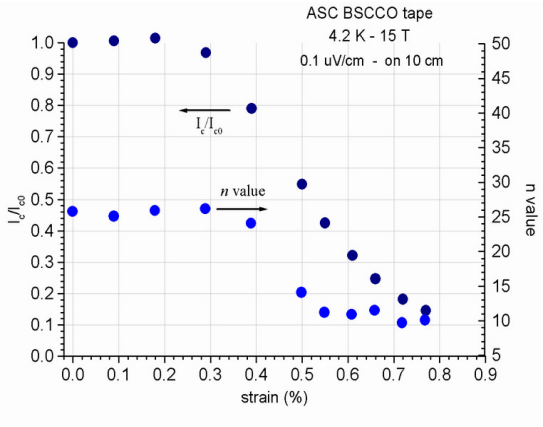

Figure 8: J_c and n factor of Ag sheathed Bi,Pb(2223) tapes as a function of strain at 4.2K and 15T.

Selected references

C. Beneduce, E. Giannini, R. Passerini, G. Witz, B. Seeber and R. Flükiger, *Phys. C* **372-376** (2002) 980.

E. Giannini, I. Savysyuk, V. Garnier, R. Passerini, P. Toulemonde and R. Flükiger, *Supercond. Sci. Technol.* **15** (2002) 1577.

R. Passerini, M. Dhallé, E. Giannini and R. Flükiger, *Supercond. Sci. Technol.* **15** (2002) 1203.

R. Passerini, M. Dhallé, B. Seeber and R. Flükiger, *Supercond. Sci. Technol.* **15** (2002) 1507.

H.L. Suo, C. Beneduce, M. Dhallé, N. Musolino, X.D. Su and R. Flükiger, *Advances in Cryogenic Engineering Materials* **488** (2002) 872.

Theory of condensed matter

Thierry Giamarchi

Research summary: The group works on the theory of condensed matter systems, in connection with various experimental groups. The activities are focussed in two main directions. One is the understanding of the effects of strong correlations in electronic systems. In particular in low dimensional systems interactions lead to non Fermi liquid states, e.g. to a Luttinger liquid in one dimension. One of the questions is to understand how to go from such states to a more conventional Fermi liquid one by coupling low dimensional systems. This question of dimensional crossover is relevant for experimental systems such as organic superconductors. Another direction of research is to understand the effect of disorder on elastic systems, both classical and quantum. Classical systems encompass vortex lattices, domain walls in magnetic or ferroelectric systems and liquid crystals. Quantum systems can be charge and spin density waves or crystals of electrons such as the Wigner crystal existing in a two dimensional electron gas at low densities. The disorder distorts the perfect lattice and leads to a glassy structure with peculiar properties (Bragg glass). It also prevents the structure to slide freely when submitted to an external force and leads to pinning. Both the static and dynamical properties of these systems are thus drastically modified by the disorder and need to be understood.

Pinned Wigner crystal

As predicted a long time ago by Wigner, if the density of an electronic system is low enough or if the kinetic energy can be blocked by a very strong external magnetic field, the electrons crystallize. This quantum crystal of electrons is a unique phase of matter with remarkable properties. This phase has thus been long searched for. Since no direct imaging of the Wigner crystal has been feasible so far, one can access the properties of this phase mostly through its transport properties, which makes it quite difficult to known whether this phase is indeed realized or not.

In the presence of disorder the competition between the interaction which wants a perfect crystal and the disorder that wants to pin the electrons randomly leads to frustration and to glassy physics. When the crystal (glass in the presence of disorder) is submitted to an external force (electric field) the disorder prevent the crystal to slide and leads to pinning. In order to ascertain whether a Wigner crystal exists or not it is thus necessary to have a theory allowing to compute the transport properties of such a system reliably.

We have developped a variational approach that allows to compute the optical longitudinal and Hall conductivities of such a Wigner crystal. This method allowed in particular to obtain the density and magnetic field dependence of the pinning peak (see Fig. 1). Our calculation shows good agreement of these dependences with the observed ones, proving that a Wigner crystal was indeed formed. We also obtain correctly an asymetric lineshape, in agreement with experiment, at variance with the Lorentzian broadening that was commonly used. Using the same approach we could compute the capacitance of a Wigner crystal system (often refered in the litterature as "compressibility").

We showed that this "compressibility" is negative and unaffected by the disorder. The negative compressibility traduces the overscreening of an external charge by the Wigner crystal.

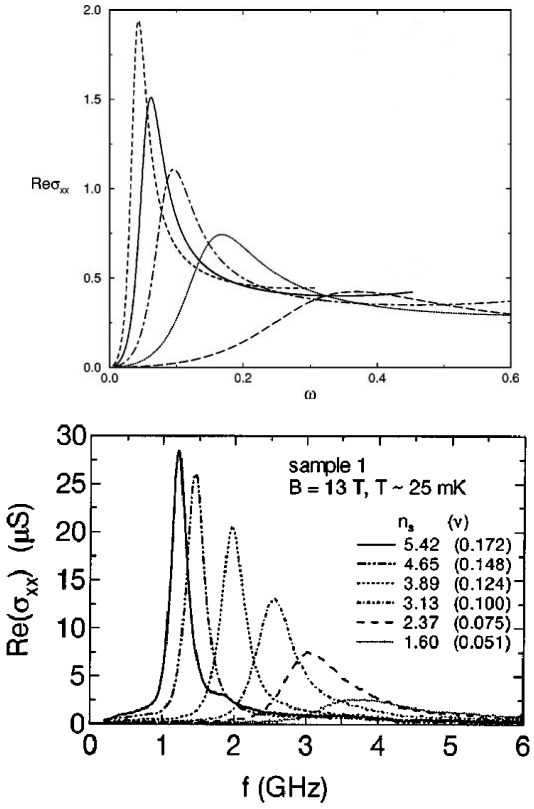

Fig.1. Calculation of the optical conductivity of a disordered Wigner crystal (top). The maximum of absorption corresponds to the pinning frequency. The lineshape and density and magnetic field dependence are in good agreement with the observed depdendence in a two dimensional electron gas under a strong magnetic field (bottom, from C. C. Li et al PRB 61 10905 (2000)).

Coupled Luttinger liquids

The effects of interactions is specially strong in low dimensional systems, in which interactions can lead to a state radically different from a Fermi liquid, the Luttinger liquid.The Luttinger liquid state is particularly relevant for organic superconductors (so called Bechgaard salts). These materials are made of coupled one dimensional chains, so it is important to know how the one dimensional physics is affected by the interchain hopping. Quite generally one can expect a dimensional crossover in which the system goes from a Luttinger liquid or one dimensional Mott insulator (for commensurate fillings) behavior at high temperature to a Fermi liquid behavior at low temperatures. Experimentally it was clearly shown that these materials are Mott insulators/Luttinger liquids at high temperature, but the dimensional crossover remained very poorly understood. We developped a mean field approach to tackle this question, by replacing the problem of coupled chains by a single chain coupled to an effective bath. This approach allows to describe the dimensional crossover and to study the physical properties of the resulting low temperature Fermi liquid phase.

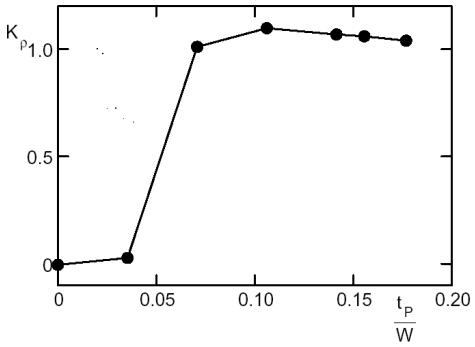

Fig.2. Solution for a system of coupled Hubbard chains. The Luttinger parameter K_ρ. goes from zero to one when the interchain hopping t_ρ is increased relatively to the intrachain bandwidth W. This is the characteristic of a transition from a one dimensional Mott insulator to a three dimensional Fermi liquid.

Creep in ferroelectrics

An elastic domain wall moving in a random media has for small driving force a very slow response, called creep, due to the fact that to move the system has to overcome diverging barriers by thermal activation. We examined, how the creep can be used to interpret data of domain wall motion in ferroelectrics. For more on this subject see J. M. Triscone's group's report.

Thermodynamics of the Bragg glass

Disorder on an elastic system leads to frustration and to glassy physics. For classical systems this physics is particularly relevant for vortex lattices or charge density wave systems that exhibit this type of competition.
As was shown a long time ago by Larkin the disorder destroys any perfect crystal below four dimension. Although it was initially believed that the destruction of the positional order in the crystal would be exponential, it was shown recently that disorder in an elastic system results in a novel glassy phase, the Bragg glass. This phase has only an algebraic decay of the positional order and perfect topological order (no defects such as dislocations at zero temperature, just as in a perfect crystal). Evidence of this phase in vortex systems has been provided recently by neutron diffraction experiments.
In connection with the physics of the Bragg glass, an interesting quantity to determine is the specific heat of such a system. Indeed understanding the behavior of the specific heat in disordered and glassy systems is a long standing problem. A general, although phenomenological interpretation was proposed assuming the existence of two level systems and led to a linear specific heat at low temperatures. Despite its remarkable success for many systems the range of applicability and microscopic justification of such a model are still open questions. Furthermore for classical system the behavior depends on whether the variables are taken to be discrete or continuous
We thus developped an approach to compute the specific heat of the Bragg glass, both in the quantum and in the classical case. For the quantum problem we find a T^3 dependance at low temperatures. We argue that this dependence is due to an hidden symmetry of the Bragg glass (statistical tilt symmetry). For the classical case we find an excess of specific heat due to the disorder, compared to the equipartition .
At low temperatures compared to melting, this correction is essentially linear in temperature, and should be observable in systems such as the vortex lattice.

For more details and further reading, see:
R. Chitra, T. Giamarchi and P. Le Doussal Phys. Rev. B 65 035312 (2002); S. Biermann et al. in ``Strongly correlated fermions and bosons in low dimensional disordered systems'', Ed. I.V. Lerner et al. (Kluwer, Dordrecht, 2002);T. Giamarchi and S. Bhattacharya, in ``High Magnetic Fields: Applications in Condensed Matter Physics and Spectroscopy'', Ed. C. Berthier et al. (Springer-Verlag, Berlin, 2002); G. Schehr, T. Giamarchi and P. Le Doussal condmat/ 0212300.

Theory and numerical physics

Bernard GIOVANNINI

Research summary: The small theory and numerical physics group in the Department has a task of working in close collaboration with the experimental groups and providing theoretical expertise, models and calculations relevant to the interpretation of actual experimental results. The group has specialized for a long time in band calculations for various complicated systems; in addition it has focussed its interest recently on developping a phenomenological model for underdoped high-temperature superconductors, based on the phase fluctuation picture of these materials, and which leads to reasonable agreement with STM and ARPES data.

Magnetism in doped systems

Many studies on doped systems, like the hexaborides, Nb in W-oxide and Mn in GaAs, have revealed weak magnetism. Vacancies of B_6 clusters in SrB_6 lead to rather large stable moments on B atoms near to the vacancy. This magnetism is of standard Stoner type and the calculations show that the moment decays rapidly with temperature. The conclusion is that this magnetism and the one near La imputities in the hexaborides are plausible, but neither one can explain the large Curie temperature. We have also calculated the electronic structures for Nb, V and Re doping in supercells of cubic WO_3, partly using the virtual crystal approximation. The results are similar to the case of La impurity in the hexaboride, so that a moment appears only when there is a larger derivative of the DOS of the impurity band, but it is the oxygens closest to the impurity that receive most of the moments.

Spin fluctuations and superconductivity in elementary metals under pressure

The recent discovery of superconductivity in iron at large pressure has led to several theoretical studies of superconducting mechanisms. We have studied the stability of three phases (fcc, bcc, and hcp) of Fe, Ni, and Co as a function of pressure, and of fcc Pd in electronic structure calculations, using the GGA potential. An analogy between perturbations of lattice distortions and of exchange splitting is used to calculate the enhancement factor for spin fluctuations, λ_{sf}, which is peaked near ferromagnetic (FM) or antiferromagnetic (AFM) instabilities, and electron-phonon coupling, λ_{ph}. For Fe we find a transition from bcc to hcp at a pressure slightly lower than the pressure at which superconductivity is observed. The results for T_c from spin fluctuations (figure) show two peaks corresponding to two

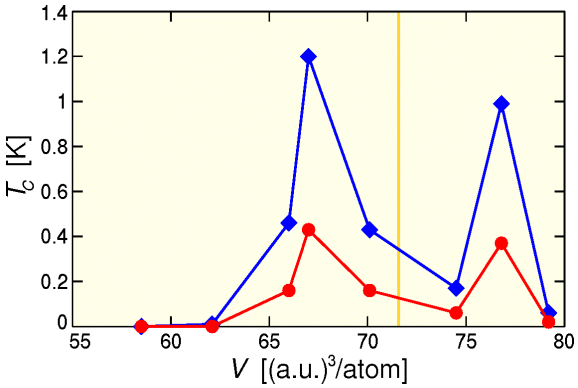

Calculated T_C for hcp iron as a function of volume. The blue line is assuming that the s part of the coupling is zero, while the red line is for equal s and d parts. The bcc phase is stable on the right-hand side of the vertical line.

AFM instabilities. The first AFM configuration occurs at a smaller pressure than the critical pressure for the bcc to hcp transition, while the results for the second one coincide fairly well with experiment, both concerning the pressure range and T_c.

The same type of calculations for Co suggests that superconductivity might be observable at very large pressure just after a hcp to fcc transition, while the bcc phase is not found to be stable. The conditions for superconductivity in Co appears here to be a bit better than for fcc Pd at ambient pressure. For the latter the calculations give a very low T_c despite the large Stoner factor for FM fluctuations.

Spin-phonon coupling in high-T_c oxides

The high-T_c materials are intriguing because their superconducting properties seem to depend both on phonons and on AFM fluctuations. Our band calculations, using the virtual crystal approximation for varying the doping in long supercells of the Hg-based high-T_c copper oxide, include both phonon distortions and spin

waves. For "half-breathing" O phonon modes, it is shown that the coupling to spin fluctuations is enhanced by the phonon and vice-versa, so that the local exchange enhancement is increased when the phonon is present and the pseudogap in the DOS coming from the charge modulation of the phonon is deeper when it coexists with the spin wave. These results are in line with many observations. The origin of pseudogaps would be the stripe-like charge and spin modulations, which are caused by selective phonon softening depending on the doping of the system. The half-breathing mode would soften zone boundary phonon involving planar oxygens. Strained and internally distorted unitcells show increased coupling in agreement with the trends from experiments with pressure and epitaxial growth as well as with correlation between T_c and the position of apical oxygens.

The strength of the enhancement factor, λ_{sf}, for spin fluctuations, calculated in the same way as for iron, varies much over the Fermi surface. But the mean value is not larger than about 0.25 for the spin wave coupled to the half-breathing mode, which is not sufficient to explain a high T_c. This problem is probably linked to the local density (LDA) potential, which finds no AF, insulating ground state of the undoped system. A staggered magnetic field with an amplitude corresponding to 23 mRy is needed to make a gap in the DOS of the undoped system. However, a slightly different localization of the bands is sufficient to reduce this critical field to almost zero. Calculations with the same parameters for the doped system confirm that the coupling is increased.

Vortex-core states

Vortex cores in type-II superconductors have been much studied during the last decades. The predicted core states were seen experimentally in several materials. However, many questions remain on the nature and properties of these states. In *d*-wave superconductors, in particular, analytical results are still lacking for core states, and the numerical calculations reported so far have raised some controversy. In order to identify the mechanism responsible for the formation of the core states, we have investigated the simplest case of an isolated *s*-wave vortex.

In *s*-wave superconductors, the formation of core states has been generally attributed to multiple Andreev scattering at the normal/superconductor boundary inside the core, suggesting that the suppression of the superconducting order in the core is the main ingredient to understand the formation of the bound states. We have found, however, that the suppression of the order

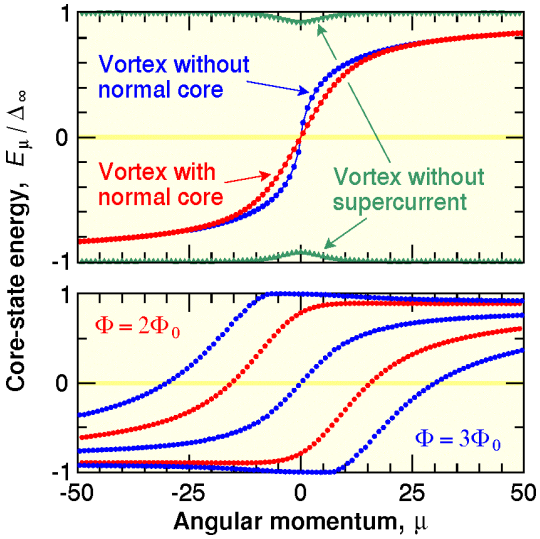

Energy spectra for various types of vortices. Top: effect of the normal core and of the supercurrent on the vortex-core spectrum. Bottom: core states in vortices carrying more than one superconducting flux quantum.

parameter has a marginal effect on the spectrum of core states. In fact, the general shape of the spectrum is determined by the strength of the supercurrent flowing around the vortex. Consequently, vortices with and without a normal core have very similar spectra (figure). The figure also shows the spectrum of a fake vortex made of a normal core but carrying no supercurrent (and thus no magnetic flux either). The spectrum is qualitatively different from the spectrum of a true vortex. In particular, there are no states at the Fermi energy in this case, and therefore no zero-bias conductance peak in the local density of states. These results prove that the order-parameter suppression alone is unable to induce a localization of the Bogoliubov quasiparticles in vortices. This conclusion applies to *d*-wave superconductors as well.

A comparison of the spectra in vortices carrying more than one flux quantum gives further evidence that the circulating superfluid plays a crucial role. In general, a vortex carrying n flux quanta has n branches of core states (figure). But only odd values of n lead to a zero-bias conductance peak in the core, i.e. to core states with both low energy *and* low angular momentum.

The main effect of the supercurrent is to change the angular momenta of the electron and hole parts of the Bogoliubov excitations. As a result, a phase difference of $n\pi/2$ is induced in the *radial* electron and hole wave functions. Thus the pairing energy can become small when the wave functions are out of phase by $\pi/2$ (odd n). This interference effect is quite different from other mechanisms leading to particle localization.

For more details and further reading, see T. Jarlborg, Physica C **385**, 513 (2003).

Specific heat and magnetocaloric effect of metals and superconductors

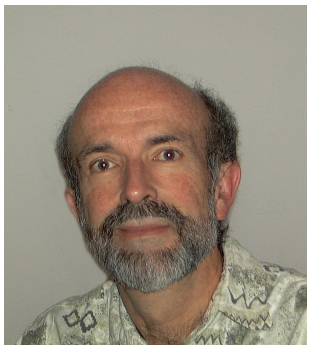

Alain JUNOD

Research summary: Our group specialises in thermodynamic studies of superconductors and new materials. In view of the preliminary results obtained in 2001, research plans were revised to concentrate on the new superconductor MgB_2. The variation of its specific heat with temperature established its two-gap structure in the bulk; that along with the magnetic field gave a tool to study two-gap vortices; finally irradiation was used to study changes in the anisotropy, which is believed to be an essential ingredient of superconductivity in MgB_2. As a volume-sensitive probe, specific heat complemented research based on surface-sensitive spectroscopies at the DPMC. Other projects made use of our sensitive equipment in calorimetry: the study of the multiple magnetic phases of UAs both by specific heat and magnetocaloric measurements came to a conclusion; some classic superconductors were revisited in view of the possible occurrence of multiple gaps. The search for pseudogap signatures in thermodynamic quantities in high temperature superconductors is going on.

Thermodynamic properties of MgB_2

The recently discovered 40 K superconductor MgB_2 shows unusual properties. Whereas it is now accepted that its superconductivity originates from conventional electron-phonon coupling, charge carriers at the Fermi level are divided into two main electronic bands with different properties. The more isotropic π band is at the origin of a smaller superconducting gap, whereas the quasi 2D σ band gives rise to a larger gap. This was shown by band-structure calculations, various spectroscopic experiments, and in particular by our specific heat (C) experiments on polycrystals. We have proceeded in two directions: i) effect of the magnetic field (H); ii) effect of disorder.

Mixed-state properties

Using polycrystals, we previously showed that the specific heat at low temperature (T) behaves abnormally: the quantity $\gamma \equiv \lim(C/T)_{T\to 0}$ increases much more rapidly with H than expected from the isotropic single band BCS (ISB) model, in a very unusual non-linear way. MgB_2, being made up of a stack of boron layers, is strongly anisotropic. A significant analysis requires single crystals; unfortunately, the synthesis of large crystals is still out of reach. We developed a microcalorimeter (Fig. 1) capable of measuring the heat capacity of an existing 39 µg single crystal from the group of S. Tajima (ISTEC, Japan).

Our new results show the existence of a cross-over field H^* ~ 0.35 T (Fig. 2). Below H^*, $\gamma(H)$ increases rapidly and isotropically, i.e. irrespective of the the orientation of H, up to about half the normal-state value. Above H^*, anisotropy sets in. This behaviour can be understood within the the two-band model, considering that π band carriers define "giant" vortex cores, i.e. much larger than would be expected from the value of the upper critical field H_{c2}. The low-T behaviour is then dominated by the contribution of the π band; our results clearly demonstrate its isotropy. These giant cores were directly observed by STM in the group of Ø. Fisher. The crossover H^* is the field at which these cores start to overlap; we may call it the virtual critical field of the π subsystem. Above H^*, the σ band carriers determine the H-dependence of γ. The vortex cores associated with these carriers are conventional, and characterized by an anisotropy of ~6, which causes that of H_{c2}. The existence of these additional field and length scales in the mixed state of MgB_2 gives rise to exciting new physics.

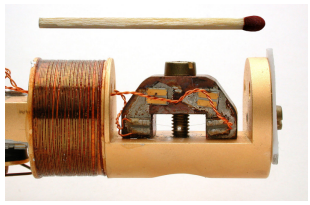

Fig.1. Microcalorimeter. The sample platform in front of the thread of the screw is a Cernox® bare chip thermometer.

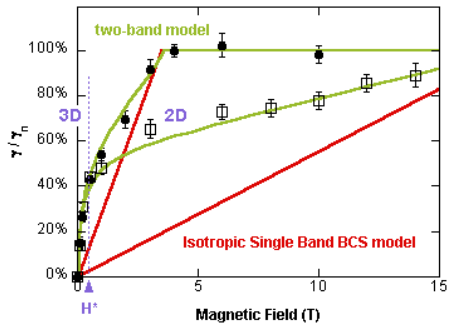

Fig.2. Normalised γ versus H for the field applied perpendicular (●, H_{c2} = 3.5 T) or parallel (□, H_{c2} = 18 T) to the boron planes. The single band model (red lines) does not fit.

Effect of irradiation

Multiple gap features are expected to be washed out by scattering. To study this phenomenon, homogeneous disorder was created in a polycrystalline sample by neutron irradiation.

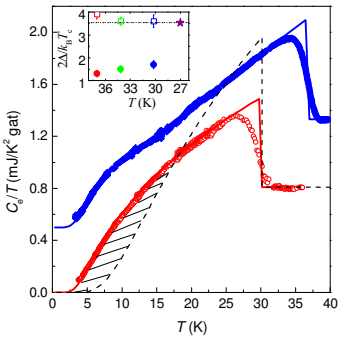

Fig.3. Electronic specifc heat of MgB_2. Top: pristine sample (shifted by 0.5 units). Bottom: sample after 2nd irradiation. Full lines: two-gap fits; dashed line: ISB curve. Inset : variation of the reduced gaps versus T_c. The symbol ★ represents the predicted BCS single gap limit.

Specific-heat measurements were performed to obtain bulk information on the evolution of either gap separately. After irradiation, T_c decreased, showing that *inter*band scattering had been introduced. We observed a suppression of the larger gap (Δ_σ), whereas the smaller one (Δ_π) remained nearly unchanged. In terms of reduced values $2\Delta/k_BT_c$, the gaps tend to converge toward the BCS single gap limit, yet slower than predicted by theory.

The large increase of H_{c2} anticipated from our measurements of $dH_{c2}/dT|_{Tc}$ was confirmed by new measurements up to 28 T (Fig. 4). This is associated with a reduction of the electronic mean free path, whereas the density of states at the Fermi level remains nearly constant.

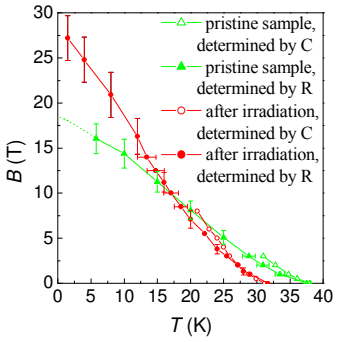

Fig. 4. Upper critical field $H_{c2}(T)$ before and after irradiation, determined by specific-heat and resistive measurements.

Magnetic phase diagram of UAs

The characterization of the magnetic phase diagram of single crystal UAs was finalized in a collaboration with the ILTSR (Wroclaw). Using our novel technique based on miniature heat-flow sensors, the region 20-160 K and 0-13 T was investigated by a mesh of orthogonal measurements of specific heat $(\delta Q/\delta T)_H$ and magnetocaloric effect $(\delta Q/\delta H)_T$. All transitions between five different magnetic structures were found to be of first-order. Their entropy jumps were estimated. We observed not only positive, but also zero and negative entropy jumps upon crossing 1st order transition lines in magneto-caloric runs, as allowed by thermodynamics. A 3D plot of the singular part of the magnetic entropy was constructed (Fig. 5). New remarkable features were observed, such as a precursor anomaly occurring ~2 T before the paramagnetic/single-**k** / ferrimagnetic transition (possibly related to the so-called Lifshitz instability), and a first-order transition without any latent heat occurring at the inversion point on the double-**k** type IA / ferri-2**k** phase transition line, bearing some analogy with the *p*-*T* phase diagram of ^{3}He.

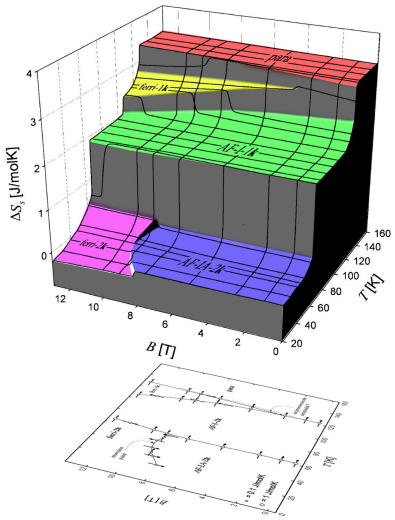

Fig.5 3D plot of the singular part of the magnetic entropy, $\Delta S_s = S_s(T, B) - S_s(20\ K, 0)$, for single-crystal UAs. The steps on the surface show the latent heat at the magnetic transitions. Each line along the T (or B) direction is a specific heat (or magnetocaloric) run. Note the inversion point at {T, B} = {46 K; 9.3 T}. The phase diagram is shown below.

Pseudogap in HTS

The observation by Kaminski *et al.* of symmetry breaking at the opening of a pseudogap (T^*) in $Bi_2Sr_2CaCu_2O_8$, a high temperature super-conductor, suggests that this is a true phase transition. A large isotope effect was reported by Temprano *et al.*, T^* = 170 K in $HoBa_2Cu_4{}^{16}O_8$ and T^* = 220 K in $HoBa_2Cu_4{}^{18}O_8$. This lead us to start a new series of differential specific heat experiments looking for a thermodynamic signature (with A. Furrer, PSI/ETHZ). Up to now only an upper limit of ±0.01% could be set for a possible anomaly in C at T^*. Further experiments are planned with $HoBa_2{}^{65}Cu_4O_8$ (T^* = 185 K).

For more details and further reading, see F. Bouquet, Y. Wang, I. Sheikin et al., Phys. Rev. Lett. **89**, 257001 (2002); F. Bouquet, Y. Wang, R. A. Fisher et al., Europhys. Lett. **56**, 856 (2001); F. Bouquet, Y. Wang, I. Sheikin *et al.*, Physica C **385**, 192 (2003); Y. Wang, F. Bouquet, I. Sheikin et al., J. Phys.: Condensed Matter **15**, 1 (2003).

Growth and electronic properties of unconventional metals and oxides

J.-M. Triscone

Research summary: Unconventional metals and oxides, including dielectric and ferroelectric insulators, ferromagnetic metals and superconductors, are studied using standard transport, local probe, and high pressure techniques. The materials investigated include single crystals, epitaxial thin films and heterostructures. In epitaxial ferroelectric films, atomic force microscopy is used to modify domain structure, to study domain wall motion, and to fabricate novel devices. Heterostructures of ferroelectric perovskites with superconducting or metallic oxides allow the realization of local field effect experiments using the nonvolatile ferroelectric polarization field, while ferroelectric / dielectric structures are used to design novel materials with tailored properties. High pressures are used to tune the electronic properties of heavy fermion systems, in particular close to phase transitions. The effect of strain on epitaxial oxide thin films is studied by applying very high hydrostatic pressures.

Disorder as the microscopic origin of domain wall creep in ferroelectric thin films

Using atomic force microscopy (AFM) to create ferroelectric domains in epitaxial $Pb(Zr,Ti)O_3$ (PZT) thin films, we have shown that domain wall motion is a creep process, with the domain wall velocity $v \propto \exp[-(1/E)^{\mu}]$ where E is the electric field driving the motion and μ a characteristic dynamical exponent related to the dimensionality of the film and the nature of the pinning potential. Our data show that μ is between 0.7 and 1. Calculations of the critical nucleus suggest that the films are in the 2D limit. Contrary to results of domain wall studies in bulk ferroelectrics, we find that the creep is a result of disorder in the sample, giving two possible models for its microscopic origins. A random bond scenario, in which defects locally change the depth of the ferroelectric double well potential, gives μ = 0.25 and μ = 0.5-0.6 for 2 and 3 dimensional films, respectively. A random field scenario, where charged defects create internal fields, locally asymmetrizing the ferroelectric double well, leads to μ = 1 for all film dimensionalities.

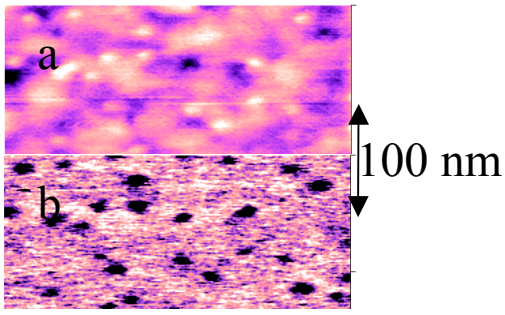

Figure 1. Topographic (a) and piezoelectric (b) AFM images of a film surface after heavy ion irradiation. The defects appear as small white mounds in the topography, and as black regions unaffected by polarization switching in the piezoelectric image.

To differentiate between these two scenarios, and to investigate their possible interplay, we are now studying films irradiated over half their surface by heavy ions, creating well defined columnar defects of known density, shown in Fig.1, whose effect on intrinsic disorder can be measured by directly comparing different regions of the sample. We are also studying domain wall roughness (Fig.2), whose characteristic exponent ζ can be independently related to μ, and which is of fundamental interest in further understanding the creep motion of ferroelectric domain walls .

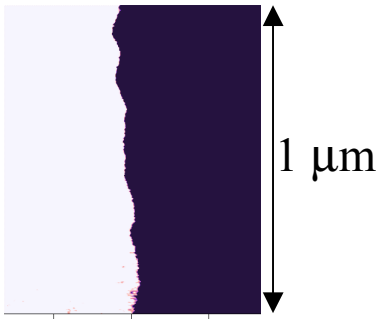

Figure 2. Piezoelectric image of a ferroelectric domain wall

For more details and further reading, see Tybell *et al.*, Phys. Rev. Lett. **89**, 097601 (2002).

Ferroelectricity in ultrathin films

Probing finite size effects is important for understanding how reduced dimensions will affect the properties of a particular material. As the physical dimensions of a ferroelectric are made smaller, it has been argued for a long time that the stability of the ferroelectric phase is altered, leading to a relatively large critical thickness required for ferroelectricity to occur. More recently, ab-initio calculations found a critical thickness of only around 26 Å (6 unit cells) for the canonical ferroelectric $BaTiO_3$[1].

Experimentally, current techniques based on a local probe approach have allowed the detection of ferroelectricity in perovskite films down to a thickness of 40 Å (10 unit cells) [2]. However, these techniques are based on the measurement of the piezoelectric signal which gets weaker as the thickness decreases, and reaches noise level below 40 Å. To test this new prediction, a technique that would allow us to probe ferroelectricity in thinner films is needed. A possible approach to studying ferroelectricity in ultrathin films is to use X-ray Photoelectron Diffraction (XPD), a technique mostly used to study the orientation of adsorbed molecules, surface segregation, and interdiffusion at interfaces. This technique yields information on the atomic structure of the surface layer, and its resolution is in theory sufficient to detect the atomic displacement related to polarization reversal. First results, shown on Fig.3, obtained with Prof. Ph. Aebi on a thin film of $PbTiO_3$ (132 Å), show that the displacements of the peaks due to the displacement of the atoms are detectable. This approach might allow us to test ferroelectricity in films a few unit cell thick.

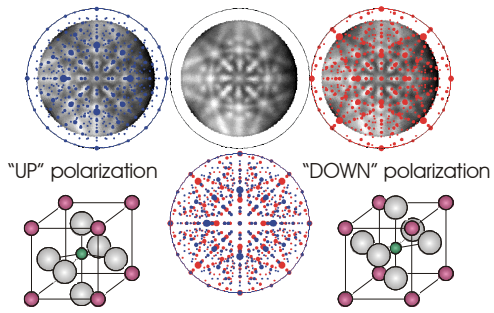

Figure 3. Angular distribution of Pb 4f photoelectrons due to forward scattering of the electrons by neighboring atoms along the crystal directions for an epitaxial thin film of $PbTiO_3$ with a mixture of both polarizations "UP" and "DOWN".

For more details and further reading, see [1] Junquera *al.*, submitted to Nature, [2] Tybell *al.*, Appl. Phys. Lett. **75**, 856 (1999).

Doped $SrTiO_3$ single crystal "thin films"

For electron doped $SrTiO_3$, *e.g.* $SrTiO_{3-x}$ and $SrTi_{1-x}Nb_xO_3$, superconductivity is found in a carrier concentration range between about 1×10^{19} and 10^{21} cm^{-3}. The critical temperature T_c depends on the carrier concentration and shows a maximum of 0.3 K at 1×10^{20} cm^{-3} [1]. This relatively low carrier concentration is clearly within the range of doping levels that have been achieved in recent ferroelectric field effect experiments[2], making doped $SrTiO_3$ an ideal candidate for model field effect studies. Here we have studied the possibility of reducing the surface of $SrTiO_3$ single crystals by using an Hydrogen Plasma Cleaning method at room temperature. The transport properties of the crystals were then measured. The doped region near the surface of the samples displayed a metallic behavior with large residual resistance ratios in the range of 100 – 1000 (see Fig.4). These values are much higher than those of bulk reduced single crystals. In these samples, we did not observe any sign of superconductivity down to 60 mK. Assuming a doped thickness of ~0.1 µm, the carrier concentration n is estimated from the Hall coefficient to be less than about 1×10^{19} $/cm^3$. Although we were not able at this time to induce superconductivity using the Hydrogen Plasma Technique, our studies suggest that the Hydrogen Plasma Cleaning method is an effective way of removing oxygen from oxide single crystal surfaces and thus "fabricating" reduced single crystal thin films.

[1]. J. F. Schooley et al., Phys. Rev. Lett. **14**, 305(1965); [2]. C. H. Ahn et al., Science **284**, 1152 (1999).

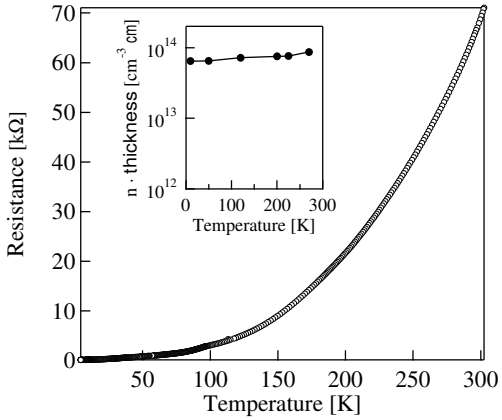

Figure 4. Temperature dependence of resistance for a $SrTiO_3$ substrate reduced by the Hydrogen Plasma Cleaning method. The inset shows the temperature dependence of the carrier concentration nx thickness.

A new field effect device based on $SrTiO_3$

We have realized a new field effect device whose gate insulator is a $SrTiO_3$ single crystal. This device allows a modulation of the critical temperature of a thin $NdBa_2Cu_3O_x$ (NBCO) layer, epitaxially deposited on the top of the $SrTiO_3$ crystal, of at least 3 Kelvin. The heterostructure used is constituted of a bilayer of an epitaxial insulating $PrBa_2Cu_3O_x$ layer deposited on top of a superconducting NBCO film, 2 unit cell thick. To realize the field effect device, we reduced the thickness of the commercial $SrTiO_3$ dielectric

single crystal substrate to about 110 microns and deposited a gold contact on the back face allowing the application of a field across the $SrTiO_3$. While applying an electric field across the dielectric, we measured the longitudinal resistivity of the NBCO path as a function of the temperature. The samples were photolithographically patterned, and measurements were performed using a standard 4 point technique. Typically, source-drain currents of 10 μA were used, while the gate leakage currents were observed to be below 1 nA. Fig. 5 shows the resistance as a function of temperature in the region of the critical temperature T_c of the NBCO layer for voltages between –200 V and 250 V applied across the $SrTiO_3$ dielectric layer. The maximum shift obtained in the critical temperature is three Kelvin whereas the maximum change in the resistance is 38%. We also characterized the dielectric properties of the gate insulator to be able to quantify the field effect. A shift of 2.1 Kelvin is obtained for an applied field of $1.8*10^6$ V/m corresponding to a polarization of 6.8 $\mu C/cm^2$. This device allows us to obtain one of the largest shift in the critical temperature obtained by field effect in oxide superconductors.

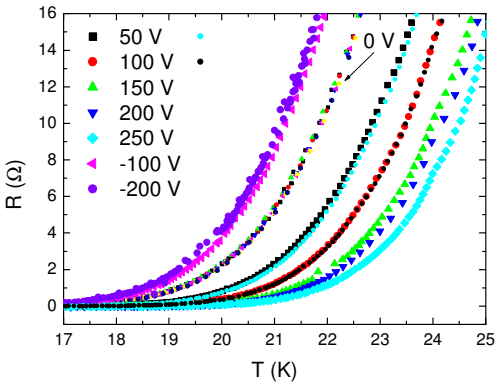

Figure 5. Resistance versus temperature of a thin NBCO layer for different voltages applied across the $SrTiO_3$ gate insulator. A shift of 2.1 Kelvin in the critical temperature is obtained between 0V and 200V corresponding to a field of $1.8*10^6$ (V/m) and a polarization of 6.8 ($\mu C/cm^2$). The maximum shift in the critical temperature between –200V and 250V is 3 Kelvin.

Superconductivity of iron at high pressure

Resistive electrical measurements on samples from three different sources show that the ε-phase of iron is superconducting in a pressure range of around 15-30 GPa. Superconductivity emerges at the martensitic bcc-hcp structural transition, i.e. at the disappearance of long-range ferromagnetic order. The onset of superconductivity has a maximum temperature of 2.5K around 20 GPa. It is only found, however, in extremely pure samples (>4N) whose mean free path is sufficiently large. We found that the superconducting state can be destroyed by mechanical work (rolling), and restored by annealing the sample (1000ºC/24h). The resistive transitions were usually incomplete, or very broad if R=0 was reached. These broad transitions resemble to flux-flow resistivity, even in the absence of an external magnetic field. One interesting possibility is that superconductivity coexists with an intrinsic field

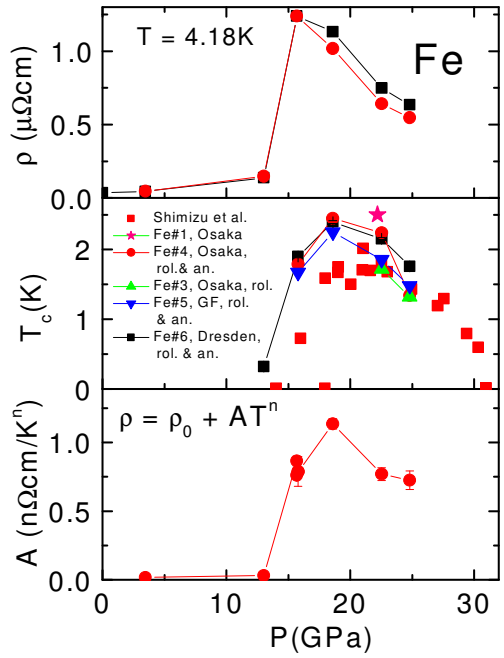

Figure 6. Pressure dependence of the superconducting transition of various Fe samples compared to the residual resistivity and A coefficient in the law $\rho = \rho_0 + AT^2$.

produced by ferromagnetic clusters remaining from the low pressure phase. The measured upper critical field is large (0.8T) and the clean limit seems to be required. The normal state resistivity follows the relation $\rho = \rho_0 + AT^n$ to around 35K with an exponent n very close to 5/3, characteristic of a nearly ferromagnetic metal. In a magnetic field greater than B_{c2}, this law persists down to low temperatures; only $\rho_0 \propto B^{\sim 3/2}$ increases. Fermi-liquid behavior ($\rho \propto T^2$) is thus never recovered. The pressure dependence of the residual resistivity ρ_0, the A coefficient, and T_c are similar: all three show a maximum around 20 GPa. The results are summarized in Fig. 6. This strong link between the normal state properties and the superconducting phase suggests that spin fluctuations play a dominant role in the formation of Cooper pairs.

Resistivity and AC-specific heat of $CeCu_2Si_2$ under high hydrostatic pressure

Last year, we reported simultaneous measurements of the resistivity and AC-specific heat of $CeCu_2Si_2$ at very high pressure and low temperature in the ideally hydrostatic He pressure medium. As shown in Fig.7, we have now explored the superconducting phase of $CeCu_2Si_2$ up to ~ 8 GPa, in conditions of temperature and pressure previously unattained with these measurement techniques. The origins of this state are still not fully understood, and the unusual non-monotonic pressure dependence of T_c has yet to be fully explained theoretically. Our recent work proved the bulk nature of the enhancement of superconductivity in $CeCu_2Si_2$, and showed its reversibility on decompression.

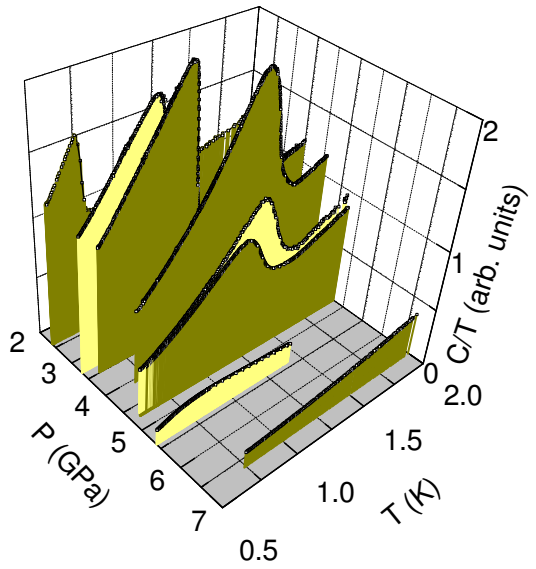

Figure 7 Evolution of the superconducting specific heat jump with pressure. Note the large enhancement at the increase in T_c, followed by a rounding of the peak and a rapid collapse as superconductivity is suppressed at high pressure.

The sharp maximum in $T_c(P)$ coincides with a number of other anomalies, including a maximum in the residual resistivity, a change in the scaling of the temperature coefficient A (where ($\rho \sim AT^n$)) versus the Kondo temperature T_K, and a maximum in the electronic specific heat γ as extracted from measurements of H_{c2}. We confirmed these observations and uncovered further anomalies at the same point. We directly observed the maximum in γ in the specific heat, and found an apparent dramatic increase in the superconducting specific heat jump, indicating a change of coupling when T_c is enhanced. This last result should be treated with caution due to the new and uncalibrated measurement technique, but it invites comparison with $CeCoIn_5$ and related compounds, where $\Delta C_p/\gamma T$ is up to five, well above the BCS value.

Resistivity and Hall effect in high quality $SrRuO_3$ thin film in the ferromagnetic state

In a previous investigation, we pressurized an epitaxial $SrRuO_3$ thin film up to 23 GPa. With increasing pressure, the Curie temperature T_C was found to decrease as in the bulk material and to saturate abruptly at 77 K above 13 GPa. We investigated a higher quality film prepared by MBE at Stanford University with a residual resistivity ratio of 50 (our previous investigations were performed on a film with a RRR of 7) in which the ferromagnetic transition in the resistivity curve is sharper and so easier to follow with increasing pressure. In all films, a crossover between two regimes is visible in the resistivity curve around 50 K, in the ferromagnetic state. In order to understand this behavior, we performed both resistivity and Hall measurements at ambient pressure for several temperatures below T_C using the van der Pauw technique up to 6 T. Above 80 K, the Hall voltage is linear in B, corresponding to an electron type carrier density of 1.5 10^{22} electrons /cm^3 in agreement with previous publication (C.H. Ahn et al., Appl. Phys. Lett. **70**, 206 (1997). With decreasing temperature below 80 K, the linear regime of the Hall voltage versus B moved progressively to a crossover with decreasing negative slope as the magnetic field is increased. Simultaneously, the extraordinary contribution to the Hall effect passes through a minimum in the same temperature region. The evolution of this behavior under pressure may provide interesting information to understand the sudden saturation observed previously in $T_c(P)$. The set-up of a similar experiment in a high pressure cell is already under way.

Selected references:

T. Tybell, P. Paruch, T. Giamarchi J.-M. Triscone, Phys. Rev. Lett. **89**, 097601 (2002).

S. Gariglio, C.H. Ahn, D. Matthey, and J.-M. Triscone, Phys. Rev. Lett. **88**, 67002 (2002).

F. Le Marrec, A. Demuer, D. Jaccard, J.-M. Triscone, M.K. Lee, C.B. Eom. Appl. Phys. Lett. **80** (2002) 2338-2340.

D. Jaccard, A.T. Holmes, G. Behr, Y. Inada, Y. Onuki. Phys. Letters A **299** (2002) 282-286.

Collaborations

Prof. P. Aebi
Université de Neuchâtel

Prof. C.H. Ahn
Yale University, USA

Dr. B. Barbiellini
Northeastern University, Boston, USA

Dr. G. Behr
Institute for Solid State and Materials Research,
Dresden, Germany

Dr. C. Beneduce
Bruker Biospin SA, Fällanden

Dr. S. Bhattacharya
NEC Research Institute, Princeton, USA

Dr. S. Biermann
LPS, Université Paris Sud, Orsay, France

Dr. N. Binggeli
ICTP, Trieste, Italie

Prof. P. C. Canfield
Ames Laboratory and Dept. of Physics and
Astronomy, Iowa State University, Ames, Iowa, USA

Prof. D. Caplin
Imperial College, London, GB

Dr. R. Chitra
LPTL, Université Paris 6, Paris, France

Dr. R. Cubitt, Dr. C. D. Dewhurst
Institut Laue-Langevin, Grenoble, France

Prof. G. Deutscher
Université de Tel Aviv, Israël

Dr M. Dhallé
Technische NatuurWetenschappen
University of Twente
Enschede, The Netherlands

Dr. S. Dugdale, Dr. G. Santi
University of Bristol, UK

Dr. B. Dutoit
EPFL, IC-LANOS, Lausanne

Dr. D. Eckert,
Bruker Biospin SA, Fällanden

Prof. C.B. Eom
University of Madison-Wisconsin, USA

Dr D. Feinberg
LEPES, Grenoble, France

Prof. J. Flouquet
CENG, Grenoble, France

Prof. Dr. A. Furrer
Laboratory for neutron scattering,
ETH Zürich and PSI Villigen

Dr. A. Georges
CNRS-LPTENS, Paris, France

Prof. R.E. Gladyshevskii
Dept. of Inorganic Chemestry
Ivan Franko National University
L'viv, Ukraine

Dr. G. Grasso
INFM Genoa, Italy

Dr. J.-C. Grivel
Risø National Laboratory
Roskilde, Denmark

Dr. B. W. Hoogenboom, M. E. Müller
Institute for Structural Biology, Universitet Basel

Dr. Y.-B. Huang
American Superconductor
Westborough, MA, USA

Dr. L.A.G.M. Jansen, Dr. J. Hinderer
Laboratoire des champs magnétiques intenses,
Grenoble, France

Prof. J.L. Jorda and Dr Ph. Galez
Laboratoire de Structure de la Matière,
Université de Savoie, Annecy, France

Dr. J. Karpinski
Laboratorium für Festkörperphysik ETH, Zürich

Prof. T. Klein
LEPES/CNRS et Université Joseph Fourier,
Grenoble, France

Prof. P. Komarek and Dr W. Goldacker
Forschungzentrum Karlsruhe, Germany

Dr. K. Kwasnitza
Paul Scherrer Institute, Villigen

Dr. A. A. Kordyuk
Institute for Solid State Research, IFW Dresden
Institute of Metal Physics of the National Academy of Sciences of Ukraine, Kyiv, Ukraine

Prof. D.C. Larbalestier
University of Wisconsin, Madison, USA

Dr. P. Le Doussal
CNRS-LPTENS, Paris, France

Dr Leghissa
Siemens AG, Erlangen, Germany

Dr. A. Lichtenstein
University of Nijmegen, The Netherlands

Prof. M. Lippmaa
Tokyo Institute of Technology, Japon

Dr. J.P. Locquet et Dr J. Fompeyrine
IBM Research Laboratory, Zürich

Dr. M. Lomello-Tafin
LAIMAN, Université de Savoie,
Annecy, France

Dr. C. Marcenat
DRFMC, Commissariat à l'énergie atomique,
Grenoble, France

Dr. C. Meingast, Dr. T. Wolf
Forschungszentrum Karlsruhe, Allemagne

Prof. K. Miyake
University of Osaka, Japan

Prof. Y. Onuki
University of Osaka, Japan

Dr. W. Paul, Dr. M. Chen
ABB Research Center, Baden-Dättwil

Dr. C. Petrovic
Brookhaven National Laboratory, Brookhaven,
New York, USA.

Prof. N.E. Phillips, Dr. R.A. Fisher
University of California and Lawrence Berkeley
National Laboratory, Berkeley, USA

Dr. T. Plackowski
Institute of Low Temperature and Structure Research,
Polish Academy of Sciences, Wroclaw, Pologne

Dr. J. W. Reiner
Yale University, USA

Dr. A. Ruyter
LEMA, Université F. Rabelais de Tours, France

Dr. G. Schehr
CNRS-LPTENS, Paris, France

Dr. B. Seeber
Groupe de Physique Appliquée,
Université de Genève

Dr. D. Sheptyakov
Paul Scherrer Institute, Villigen

Dr C. Simon
Laboratoire CRISMAT, Caen, France

Prof. A.S. Siri
University of Genoa, Italy

Dr. S. Spreafico
Pirelli Cavi e Sistemi S.p.A., Milano, Italy

Profs. P. Stadelmann and P. Buffat
EPFL, Lausanne

Prof. S. Tajima, Dr. S. Lee
Superconductivity Research Laboratory, ISTEC,
Tokyo, Japon

Dr. S. Tanaka
Kansai Advanced Research Center,
Communications Research Laboratory, Japan

Dr. B. Ten Haken
Technical University Twente, Enschede
The Netherlands

Prof. H. Ten Kate
CERN, Geneva

Dr. P. Tixador and Dr. L. Porcar
CNRS – CRTBT, Grenoble, France

Dr P. Toulemonde
LPMCN**,** Université Claude Bernard
Lyon-I, Villeurbanne France

Prof. H.W. Weber, Dr. M. Eisterer
Atominstitut der österreichischen Universitäten,
Vienne, Autriche

Dr. F. Weiss
LMPG, Grenoble, France

Dr. H. Wilhelm
Max-Planck-Institut, Dresden, Germany

Publications

Abächerli V., Uglietti D., Seeber B., and Flükiger R. (*Nb,Ta,Ti)$_3$ Sn multifilamentary wires using Osprey bronze with high tin content and NbTa/NbTi composite filaments*. Physica C **372-376**,1325-1328 (2002).

Antognazza L., Decroux M., Reymond S., de Chambrier E., Paul W., Chen M., and Fischer Ø. *Simulation of the behavior of superconducting YBCO lines at high current densities.* Physica **C372-376**, 1684 (2002).

Aoki D., Huxley A., Ressouche E., Sheikin I., Flouquet J., Brison J.P., and Paulsen C., *Superconductivity in two itinerant uranium ferromagnets: UGe$_2$ and URhGe*, J. Phys. Chem. Solids **63**, 1179-1182 (2002).

Beneduce C., Giannini E., Passerini R., Witz G., Seeber B. and Flükiger R. *Hot isostatic pressure reaction treatment of Ag-sheathed Bi, Pb(2223) tapes.* Physica C **372-376**, 980-983 (2002).

Biermann S., Georges A., Giamarchi T. and Lichtenstein A. *Quasi-one-dimensional organic conductors: dimensional crossover and some puzzles. In: "Strongly correlated fermions and bosons in low dimensional disordered systems",* Ed. I.V. Lerner et al., Kluwer (Dordrecht), 2002.

Bouquet F., Wang Y., Sheikin I., Plackowski T., Junod A., Lee S., and Tajima S. *Specific Heat of Single Crystal MgB$_2$: A Two-Band Superconductor with Two Different Anisotropies.* Phys. Rev. Lett. **89**, 257001-(1-4) (2002).

Bouquet F., Fisher R.A., Phillips N.E., Hinks D.G., and Jorgensen J.D. *Specific heat of Mg^{11}B$_2$, a two gap superconductor*. J. Superconductivity **15**, 469-473 (2002).

Chitra R., Giamarchi T. and Le Doussal P. "*Pinned Wigner Crystals*", Phys. Rev. B **65**, 035312 (2002).

Demuer A., Jaccard D., Sheikin I., Raymond S., and Flouquet J. *Pressure tuning through the magnetic instability of CePd$_2$Si$_2$*, Physica B **312-313**, 418-419 (2002).

Demuer A., Holmes A.T., Jaccard D. *Strain enhancement of superconductivity in CePd$_2$Si$_2$ under pressure*. J. Phys.: Condens. Mat. **14**, L529-L535 (2002).

Eskildsen M.R., Kugler M., Tanaka S., Jun J., Kazakov S.M., Karpinski J. and Fischer Ø., *Vortex Imaging in the π Band of Magnesium Diboride*. Phys. Rev. Lett. **89**, 187003 (2002).

Fisher R.A., Bouquet F., Phillips N.E., Hinks D.G., and Jorgensen J.D. *Identification and Characterization of Two Energy Gaps in Superconducting MgB$_2$ by Specific-Heat Measurements*. In: Studies of High Temperature Superconductors, editor A.V. Narlikar, Nova Publishers, Commack (N.Y.) **38,** 207-219 (2002).

Fisher R.A., Bouquet F., Phillips N.E., Hinks D.G., and Jorgensen J.D. *Specific heat of Mg^{11}B$_2$ in magnetic fields: two energy gaps in the superconducting state*. Int. J. Modern Phys. B **16**, 3180-3183 (2002).

Fisher R.A., Bouquet F., Phillips N.E., Hundley M.F., Pagliuso P.G., Sarrao J.L., Fisk Z., and Thompson J.D. *Specific heat of CeRhIn$_5$: Pressure-driven evolution of the ground state from antiferromagnetism to superconductivity*. Phys. Rev. B **65**, 224509-(1-6) (2002).

Fisher R.A., Bouquet F., Phillips N.E., Hundley M.F., Pagliuso P.G., Sarrao J.L., Fisk Z., and Thompson J.D. *Specific Heat of CeRhIn$_5$: Pressure-Driven Transition From Antiferromagnetism to Heavy-Fermion Superconductivity.* J. Superconductivity **15**, 433-438 (2002).

Franck J.P., Isaac I., Zhang G., Gordon J.E., Marcenat C., Lortz R., Meingast C., Bouquet F., Fisher R.A., and Phillips N.E. *A Study of the Paramagnetic to Ferromagnetic Transition in the Optimally Doped CMR Compound La$_{0.65}$Ca$_{0.35}$MnO$_3$ and its Dependence on Oxygen Mass*. J. Superconductivity **15**, 571-577 (2002).

Gariglio S., Ahn C.H., Matthey D., and Triscone J.-M. *Electrostatic tuning of the hole density in NdBa$_2$Cu$_3$O$_{7-\delta}$ films and its effect on the Hall response.* Physical Review Letters **88**, 67002 (2002).

Giamarchi T. and Bhattacharya S. *Vortex Phases.* In: "High Magnetic fields : applications in condensed matter physics and spectroscopy", Ed. C. Berthier et al., Springer Verlag 2002.

Giamarchi T. "*Disordered Wigner crystals*". In: "Strongly correlated fermions and bosons in low dimensional disordered systems", Ed. I.V. Lerner et al., Kluwer (Dordrecht), 2002.

Giannini E., Savysyuk I., Garnier V., Passerini R., Toulemonde P. and Flükiger R. *Reversible melting and equilibrium phase formation of (Bi,Pb)$_2$Sr$_2$Ca$_2$Cu$_3$O$_{10+\delta}$*,. Supercond. Sci. Technol. **15,** 1577-1586 (2002).

Giannini E., Passerini R., Toulemonde P., Walker E., Lomello-Tafin M., Sheptyakov D. and Flükiger R. *Bi,Pb(2223) equilibrium and decomposition: in situ high-temperature neutron diffraction study*. Physica C **372-376,** 895-898 (2002).

Gordon J.E., Marcenat C., Franck J.P., Isaac I., Guanwen Zhang, Lortz R., Meingast C., Bouquet F., Fisher R.A., and Phillips N.E. *Specific Heat and Thermal Expansion of La$_{0.65}$Ca$_{0.35}$MnO$_3$: Magnetic-Field Dependence, Isotope Effect, and Evidence for a First-Order Phase Transition*. Phys. Rev. B **65**, 024441-(1-4) (2002).

Grévin B., Maggio-Aprile I., Bentzen A., Kuffer O., Joumard I. and Fischer Ø. *Scanning tunneling potentiometry search for mesoscopic phase separation in $La_{0.7}Sr_{0.3}MnO_3$*. Appl. Phys. Lett. **80**, 3979 (2002).

Hoogenboom B.W., Renner Ch., Maggio-Aprile I. and Fischer Ø. *Scanning tunneling spectroscopy on vortex cores in high-Tc superconductors*. In: Vortices in unconventional superconductors and superfluids, R. P. Huebener, N. Schophohl and G. E. Volovik (eds.), Springer series in solid-state science **132**, 269 (2002).

Jaccard D., Holmes A. T., Behr G., Inada Y., Onuki Y. *Superconductivity of ε-Fe: complete resistive transition.* Phys. Letters A **299**, 282-286 (2002).

Jarlborg T. *Ferromagnetic and antiferromagnetic spin fluctuations and superconductivity in the hcp-phase of Fe*. Phys. Lett. A **300**, 518-523 (2002).

Jarlborg T. *Spin-phonon interaction in doped high-T_c superconductors from density functional calculations*. Phys. Lett. A **295**, 154-159 (2002).

Jarlborg T. *Spin fluctuations, electron-phonon coupling and superconductivity in near-magnetic elementary metal - Fe, Co, Ni and Pd*. Physica C **385**, 513-524 (2003).

Junod A., Wang Y., Bouquet F., and Toulemonde P. *Specific heat of the 38-K superconductor MgB_2 in the normal and superconducting state: bulk evidence for a double gap*. In: *Studies of High Temperature Superconductors*, editor A.V. Narlikar, Nova Publishers, Commack (N.Y.) **38**, 179-205 (2002).

Le Marrec F., Demuer A., Jaccard D., Triscone J.-M., Lee M.K., Eom C.B.. *Magnetic behavior of epitaxial $SrRuO_3$ thin films under pressure up to 23 GPa.* Appl. Phys. Lett. **80**, 2338-2340 (2002).

Matthey D., Gariglio S., Ahn C.H., and Triscone J.-M. *Electrostatic modulation of the superconducting transition in thin $NdBa_2Cu_3O_{7-\delta}$ films: the role of classical fluctuations*. Physica **C 372-376**, 583 (2002).

Passerini R., Dhallé M., Giannini E., and Flükiger R. *SEM investigation of outgrowths formation mechanism in Ag-sheathed Bi,Pb(223) tapes*. Supercond. Sci. Technol. **15**,1203-1212 (2002).

Passerini R., Dhallé M., Seeber B., and Flükiger R. *Mechanical properties of Bi,Pb(2223) single filaments and $I_c(\varepsilon)$ behaviour in longitudinally strained tapes*. Supercond. Sci. Technol. **15**, 1507-1511 (2002).

Plackowski T., Wang Y., and Junod A., *Specific heat and magnetocaloric effect measurements using commercial heat-flow sensors*, Re. Sci. Instrum. **73**, 2755-2765 (2002).

Reymond S., Antognazza L., Decroux M., Koller E., Reinert P. and Fischer Ø. *Current-induced highly dissipative domains in high-Tc thin films*. Phys. Rev. B **66**, 14522 (2002).

Sheikin I., Wang Y., Bouquet F., Lejay P., and Junod A., *Specific heat of heavy-fermion $CePd_2Si_2$ in high magnetic fields*, J. Phys.: Condensed Matter **14,** L543-549 (2002).

Su X.-D., Witz G., Kwasnitza K. and Flükiger R., *Fabrication of square and round Ag/Bi(2223) wires and their ac loss behaviour*. Supercond. Sci. Technol. **15**, 1184-1189 (2002).

Su X.-D., Witz G., Passerini R., Kwasnitza K. and Flükiger R. *Square and round Bi(2223) wire configurations and their AC losses.* Physica C **372-376,** 942-944 (2002).

Suo H.L., Beneduce C., Dhallé M. , Musolino N., Su X.-D. and Flükiger R. *High transport and inductive critical currents in dense Fe- and Ni-Clad MgB_2 tapes using fine powder*. Advances Cryogenic Engineering Materials **488,** 872-879 (2002).

Suo H.L., Genoud J.-Y., Caracino P., Spreafico S., Schindl M., Walker E. and Flükiger R. *Mechanically reinforced $\{110\}\langle 110\rangle$ textured Ag/Ni-alloys composite substrates for low-cost coated conductors.* Physica C **372-376**, 835-838 (2002).

Suo H.L., Beneduce C., Su X.-D. and Flükiger R. *Fabrication and transport critical currents of multifilamentary MgB_2/Fe wires and tapes*. Supercond. Sci. Technol. **15,** 1058-10 (2002).

Tybell T., Paruch P., Giamarchi T. and Triscone J.-M. *Domain wall creep in epitaxial $Pb(Zr_{0.2}Ti_{0.8})O_3$ thin films.* Physical Review Letters **89**, 097601-1 (2002).

Tybell T., Paruch P. Ahn Ch.H., and Triscone J.-M. *Nanoscale study of polarization phenomena in $Pb(Zr_{0.2}Ti_{0.8})O_3$ thin films*. In "Superconducting and related Oxides: Physics and Nanoengineering V", Proceedings of SPIE, volume 4811, 256 (2002).

Vidal J., Mouhanna D. and Giamarchi T. *Interacting fermions in self-similar potentials*. Phys. Rev. B **65**, 014201 (2002).

Wilhelm H., Jaccard D. *Alternative current calorimetry at very high pressure and low temperature*. J. Phys.: Condens. Matter.**14**, 10683-10687 (2002).

Wilhelm H., Jaccard D. *Calorimetric and transport investigations of $CePd_{2+x}Ge_{2-x}$ (x=0 and 0.02) up to 22 GPa.* Phys. Rev. B **66**, 64428-1-64428-9. (2002).

Witz G., Su X.-D., Kwasnitza K., Dhallé M., Beneduce C., Passerini R., Giannini E. and Flükiger R. *Reduction of AC losses in Bi-Pb(2223) tapes by the introduction of barriers and the use of new wire configurations.* Physica C **372-376**, 1814-1817 (2002).

Accepted for publication

Bellingeri E. B3.2.3 – *Processing of high T_c conductors: the compound Tl(1223)*. To appear in "Handbook of Superconducting Materials, Volume 1, edited by D. Cardwell and D. Ginley, IOP Publishing Ltd., 2003, Bristol and Philadelphia.

Bellingeri E. and Flükiger R. *C3 – TIBCCO*. To appear in "Handbook of Superconducting Materials", Volume 1, Superconductivity, Materials and Processes, edited by D. Cardwell and D. Ginley, IOP Publishing Ltd., 2003, Bristol and Philadelphia.

Berthod C., Binggeli N., and Baldereschi A. *Schottky barrier heights at polar metal/semiconductor interfaces.* Phys. Rev. B (2003).

Bouquet F., Wang Y., Sheikin I., Toulemonde P., Eisterer M., Weber H.W., Lee S., Tajima S., and Junod A. *Unusual effects of anisotropy on the specific heat of ceramic and single crystal MgB_2*. To appear in Physica C, special issue devoted to MgB_2.

Decroux M., Antognazza L., Reymond S., Paul W., Chen M., and Fischer Ø. *Studies of YBCO strip lines under voltage pulses: optimisation of the design of fault current limiters.* Accepted for publication in IEEE Trans. On Applied Superconductivity.

Demuer A., Holmes A.T., Jaccard D. *Effect of anisotropic strain on the electronic properties of the pressure incuced superconductor $CePd_2Si_2$.* To appear in Acta Phys. Pol. B, February 2003 (Proceedings of the SCES02 conference).

Eskildsen M.R., Kugler M., Levy G., Tanaka S., Jun J., Kazakov S.M., Karpinski J. and Fischer Ø. *Vortex lattice imaging in single crystal MgB_2 by scanning tunneling spectroscopy*. To appear in Physica C.

Eskildsen M.R., Kugler M., Levy G., Tanaka S., Jun J., Kazakov S.M., Karpinski J. and Fischer Ø. *Scanning Tunneling Spectroscopy on Single Crystal MgB_2*. To appear in Physica C.

Fisher R.A., Li G., Lashley J.C., Bouquet F., Phillips N.E., Hinks D.G., Jorgensen J.D., and Crabtree G.W. *Specific Heat of $Mg^{11}B_2$*. To appear in Physica C, special issue devoted to MgB_2.

Fisher R.A., Bouquet F., Phillips N.E., Hundley M.F., Pagliuso P.G., Sarrao J.L., Fisk Z., and Thompson J.D. *Specific Heat of $CeRhIn_5$ Under Pressure to 21 kbar: Pressure-Driven Transition from Antiferromagnetism to Heavy-Fermion Superconductivity.* Proceedings of the 23rd Int. Conf. on Low Temp. Phys., Hiroshima (Japan) 20-27 Aug. 2002. To appear in Physica C.

Flükiger R., Lezza P., Beneduce C, Musolino N. and Suo H.L. *Improved transport critical current and irreversibility fields in mono- and multifilamentary Fe/MgB_2 tapes and wires using fine powders*. Supercond. Sci.Technol., in press.

Flükiger R., Suo H.L., Musolino N., Beneduce C., Toulemonde P. and Lezza P. *Superconducting properties of MgB_2 tapes and wires*. Physica C, in press.

Flükiger R. *B2.5 – Growth of A15 type single crystals and polycrystals and their physical properties.* To appear in "Handbook of Superconducting Materials", Volume 1, Superconductivity, Materials and Processes, edited by D. Cardwell and D. Ginley, IOP Publishing Ltd, Bristol and Philadelphia.

Flükiger R. *B3.3.1 – Overview of low T_c materials for conductor applications*. To appear in "Handbook of Superconducting Materials", Volume 1, Superconductivity, Materials and Processes, edited by D. Cardwell and D. Ginley, IOP Publishing Ltd, Bristol and Philadelphia.

Giannini E., Garnier V., Savysyuk I., Passerini R., Witz G., Su X.-D., Seeber B., Hua L. and Flükiger R. *"Partial melting and HIP processing of Bi(2223): bulk and tapes".* Accepted for publication in IEEE Transactions on Applied Superconductivity.

Holmes A., Demuer A, Jaccard D., *Resistivity and AC-calorimetric measurements of the superconducting transition in $CeCu_2Si_2$ under very high hydrostatic pressure in a helium-filled diamond anvil cell.* To appear in Acta Phys. Pol. B, February 2003 (Proceedings of the SCES02 conference).

Hoogenboom B. W., Berthod C., Peter M., Fischer Ø., and Kordyuk A. A. *Modeling scanning tunneling spectra of $Bi_2Sr_2CaCu_2O_{8+\delta}$*. Phys. Rev. B (2003).

Jarlborg T. *Temperature dependence of magnetism near defects in SrB_6*. J. Phys.: Condens. Matter, Letter (2003).

Jarlborg T. *Electronic structure and magnetism in $X_xW_{1-x}O_3$ (X=Nb, V, Re) from supercell calculations*. J. Magn. Magn. Mater. (2003).

Junod A., Wang Y., Bouquet F., Toulemonde P., Eskildsen M.R., Eisterer M., Weber H.W., Lee S., and Tajima S. *Specific heat of ceramic and single crystal MgB_2*. Proceedings of the 23rd Int. Conf. on Low Temp. Phys., Hiroshima (Japan) 20-27 Aug. 2002, to appear in Physica C.

Karpinski J., Angst M., Jun J., Kazakov S.M., Puzniak R., Wisniewski A., Roos J., Keller H., Perucchi A., Degiorgi L., Eskildsen M.R., Bordet P., Vinnikov L. and Mironov A. *MgB_2 single crystals: high pressure growth and physical properties*. To appear in Supercond. Sci. Technol.

Matthey D., Gariglio S., Ahn C.H. and Triscone J.-M. *Field effect and ferroelectric field effect in correlated oxide films.* To appear in the Proceedings of the SPIE 2002 conference, Seattle, USA.

Murakami M. and Flükiger R. *B1 - Introduction to processing methods*. To appear in: "Handbook of Superconducting Materials", Volume 1, Superconductivity, Materials and Processes, edited by D. Cardwell and D. Ginley, IOP Publishing Ltd., 2003, Bristol and Philadelphia,

Paruch P., Tybell T., and Triscone J.-M. *Nanoscale control and domain wall dynamics in epitaxial ferroelectric $Pb(Zr_{0.2}Ti_{0.8})O_3$ thin film*s. To appear in the Proceedings of the CIMTEC 2002 conference, Firenze, Italy.

Phillips N.E., Bouquet F., Fisher R.A., Hinks D.G., and Jorgensen J.D. *Specific Heat of $Mg^{11}B_2$: Evidence for a Second Energy Gap.* Proceedings of the 23rd Int. Conf. on Low Temp. Phys., Hiroshima (Japan) 20-27 Aug. 2002. To appear in Physica C.

Phillips N.E., Fisher R.A., Bouquet F., Hundley M.F., Pagliuso P.G., Sarrao J.L., Fisk Z., and Thompson J.D. *Specific Heat of $CeRhIn_5$: Pressure-Driven Transition from Antiferromagnetism to Heavy-Fermion Superconductivity.* To appear in J. Phys.: Condensed Matter.

Plackowski T., Junod A., Bouquet F., Sheikin I., Wang Y., Jezowski A., and Mattenberger K., *Specific heat and isothermal magnetocaloric effect for single-crystal UAs*. To appear in Phys. Rev. B.

Sheikin I., Gröger A., Raymond S., Jaccard D., Aoki D., Harima H., and Flouquet J. *High magnetic field study of $CePd_2Si_2$*. Accepted in Phys. Rev. B.

Suo H.L., Toulemonde P. and Flükiger R. *B3.3.6 – Processing of low T_c conductors: the compound MgB_2*. To appear in "Handbook of Superconducting Materials", Volume 1, Superconductivity, Materials and Processes, edited by D. Cardwell and D. Ginley, IOP Publishing Ltd, Bristol and Philadelphia,

Toulemonde P., Musolino N. and Flükiger R. *High pressure synthesis of pure and doped superconducting MgB_2 compounds.* Supercond. Sci. Technol., in press

Wang Y., Bouquet F., Sheikin I., Toulemonde P., Revaz B., Eisterer M., Weber H.W., Hinderer J., and Junod A. *Specific heat of MgB_2 after irradiation.* J. Physics: Condensed Matter **15**, 1-11 (2003).

Ph.D. Thesis

HOOGENBOOM Bart W.
Scanning Tunneling Spectroscopy on Vortex Cores in $Bi_2Sr_2CaCu_2O_{8+\delta}$
September 2002